Performance of low-cost indoor air quality monitors for $PM_{2.5}$ and PM_{10} from residential sources

Zhiqiang Wang[1], Woody W. Delp[2], Brett C. Singer[2*],

[1] Tianjin Key Lab of Refrigeration, Tianjin University of Commerce, Tianjin, China

[2] Indoor Environment Group and Residential Building Systems Group, Lawrence Berkeley National Laboratory, Berkeley, CA, USA

*Corresponding email: bcsinger@lbl.gov

Acknowledgements

This research was supported by the Building America Program and the U.S.–China Clean Energy Research Center – Building Energy Efficiency Program, both within the Building Technologies Office of the U.S. Department of Energy, and was conducted at LBNL under Contract No. DE-AC02-05CH1123. Additional support was provided by the U.S. Environmental Protection Agency Indoor Environments Division through Interagency Agreement DW-89-9232201-7. Dr. Wang was supported by the National Key Project of the Ministry of Science and Technology, China through Grant No. 2016YFC0207101. We thank Marion Russell and student assistants for contributions to the filter analysis and Michael Sohn for his helpful comments.

Abstract

Advances in particle sensor design and manufacturing have enabled the development of low-cost air quality monitors (LCMs). The sensors use light scattering to estimate mass concentration and thus require evaluation for aerosols of varied composition and size distribution. We tested the performance of six LCMs designed for home use and having a retail price under US$300 in October 2018. We assessed their performance by comparing their output to reference $PM_{2.5}$ and PM_{10} measurements from 21 common residential sources and from infiltrated outdoor $PM_{2.5}$. Reference data were obtained by using gravimetric measurements to adjust time-resolved output from an aerosol spectrometer with both electrical mobility and optical particle sensors. Compared by linear regression to reference measurements, LCMs had negative intercepts and slopes of 1-2

for infiltrated outdoor $PM_{2.5}$. Semi-quantitative responses (~50–200% of actual $PM_{2.5}$) were obtained for varied aerosols including minerals (ultrasonic humidifier, vacuuming, test dust); combustion products (incense, mosquito coil, extinguished candles); microwave popcorn; and cooking involving frying or grilling. LCMs had low or no response to sources for which all mass was in particles smaller than 0.25 μm, including steady candle flames and cooking without frying or grilling. PM_{10} data from LCMs was more variable than $PM_{2.5}$.

Key Words: Combustion; Consumer IAQ monitor; Cooking; Exposure; Intervention; Source control.

1. Introduction

Adverse health effects from fine particulate matter inhalation is a global health concern. A U.S. Environmental Protection Agency[1] review concluded that increased exposure to ambient particles smaller than 2.5 μm in diameter, $PM_{2.5}$, causes increased cardiovascular morbidity and mortality, and likely causes increased respiratory illness. Much exposure to ambient $PM_{2.5}$ occurs in residences, where we are also exposed to particles emitted by activities including smoking, cooking, burning incense and candles, crafts, and settled dust re-suspension. Indoor air quality (IAQ) monitoring can provide feedback on efforts to protect occupants from infiltrating (high) outdoor $PM_{2.5}$, help to identify indoor activities that generate PM[2, 3], or automatically activate ventilation or filtration when readings exceed a designated threshold[4]. The potential to incorporate IAQ monitoring into smart home management systems is receiving increasing attention[5, 6].

A common standard for $PM_{2.5}$ measurement is the U.S. EPA's gravimetric Federal Reference Method[7, 8] (FRM). The time resolution of filter-based sampling is constrained by the need to collect enough particles to reliably discern a change in filter mass and the high cost of weighing and handling filters. To enable higher time resolution regulatory monitoring, the US EPA offers a Federal Equivalent Method (FEM) designation that is obtained by demonstrating correlation to an FRM when sampling ambient aerosols[8]. FEM monitors offer hourly or better resolution.

Even higher time resolution (minute scale or better) is achieved by devices that estimate particle concentrations based on light scattering, utilizing either photometry or optical particle counting. In photometry, the scattered light from an ensemble of particles passing through the sensor cell is translated to mass concentration based on a reference calibration[9, 10]. Since photometers require calibration to the specific aerosol of interest, some professional grade models include onboard filter sampling. Optical particle counters (OPCs) use assumptions about particle shape and refractive index to calculate the size of each individual particle that scatters laser light while passing through the sensor cell. Particles are assigned to size bins and mass concentrations are estimated using assumptions about density or through calibration to reference measurements[9]. Many published studies on time-resolved $PM_{2.5}$ in occupied homes have used photometers or optical particle counters[11-19]. Several studies have reported large variations in the calibration or response factors for professional grade optical monitors measuring aerosols relevant to residential $PM_{2.5}$, and variations of 30–50% over time for some sources.[13, 20-22]

Real-time monitoring of fine particles within homes is now possible with devices that utilize mass produced optical sensors and cost under US$300. Low-cost monitors (LCM), described elsewhere as "consumer grade"[22, 23], vary in their reporting interface (e.g., on device or via cell phone), time-resolution of data reporting, and their ability to communicate with control equipment using smart home platforms. Particle levels may be reported in mass concentration units ($\mu g\ m^{-3}$), as particle number concentrations, as an air quality index (AQI) or as a score on a proprietary scale.

There is a rapidly growing literature on the performance of low-cost sensors and monitors for ambient particles[24], but fewer studies focusing on IAQ. In ambient studies, sensors are compared against regulatory monitoring equipment over weeks to months[25-37], and some have proposed sophisticated algorithms to account for humidity and other environmental factors[38]. The most extensive and systematic evaluations have been done by the South Coast Air Quality Management District's Air Quality Sensor Performance Evaluation Center (AQ-SPEC) (www.aqmd.org/aq-spec) using methods described in a recent paper[39]. The US EPA also provides resources via their sensor toolbox website (www.epa.gov/air-sensor-toolbox).

For aerosols relevant to residential exposures, Dacunto et al.[40] reported calibration factors to relate output of the Dylos DC1100 monitor to gravimetric measurements for 17 common residential particle sources. Manikonda et al.[41] evaluated several monitors (AirAssure, AB AirSense, Dylos, Speck) measuring cigarette smoke and Arizona Test Dust in a room-sized chamber. Singer and Delp reported response factors for seven monitors (AirBeam, Air Quality Egg, AirVisual Node, Awair, Foobot, Purple Air PA-II, Speck) measuring various residential sources in a lab[22]. Zou et al. compared output of 3 bare sensors and 5 devices (not identified) to reference measurements for 27 emission events in a house[42]. Curto studied two monitors (HAPEX Nano and TZOA) measuring wood smoke leakage from fireplaces in U.S. homes and cooking in Indian homes[43]. Zamora et al. evaluated the Plantower PMS A003 with cooking emissions in a small apartment[37]. Wang et al.[44] and Sousan et al.[45] systematically studied the performance of low-cost sensors measuring particles of varying sizes and compositions in controlled laboratory testing.

The objective of this study was to evaluate the performance of LCMs (of 2018 vintage) for measuring common residential sources of fine particles. The approach largely follows a 2017 study[22] that reported semiquantitative (within 2x actual) responses of four monitors to most of the sources tested, very low or inconsistent responses of 3 monitors, and an inability of all the monitors to detect emission events that were comprised entirely of particles with optical diameters of <0.3 μm. Specific drivers of the current study were the availability of updated versions of three monitors (Awair2, Air Quality Egg 2018, and AirVisual Pro) tested previously, an indoor version of the Purple Air (PAI), and two monitors not previously evaluated (Kaiterra Laser Egg 2 and Ikair).

2. Method

2.1. Low-cost monitor selection

Candidate monitors were identified from recent review papers[46, 47] and by searching internet marketplaces for combinations of the terms (meter or monitor) and (indoor air quality, air quality, dust, particle, or PM). Monitors selected for testing met these criteria: (1) has sensor for $PM_{2.5}$, “fine particulate matter” or “fine particles”; (2) reported particle mass concentrations, not

only AQI; (3) has internal data logging or accessible cloud storage at 5-min or better resolution; (4) displays real-time data on device or mobile app; and (5) available for retail purchase in the U.S. or China in October 2018 at cost of US$300 or less. Any device previously determined to have inconsistent correlation to reference monitors in published third party testing was excluded unless it had been updated to address the performance issue. The six monitors shown in Table 1 were selected and purchased.

2.2. Reference measurements

Reference measurements were obtained using a Tapered Element Oscillating Microbalance (TEOM) with Filter Dynamic Measurement System (FDMS) (Model 1405-DF, Thermo Fisher Scientific), and by collecting filter samples for gravimetric analysis. The FDMS version of the TEOM is an FEM that intermittently (a) collects sample onto a microbalance filter for mass concentration determination, then (b) draws filtered air over the microbalance filter to quantify any gain or loss from semivolatile compounds. The configuration and processing of TEOM output to obtain 6-min resolved data is described in the Supplementary Material (SM). Gravimetric samples were collected using 37 mm diameter, 2 μm pore-size, TEFLO (Pall) PTFE filters and two AirCon2 High Volume Air Samplers (Sensidyne) at target flow rates of 10.0 lpm. The flow was checked before each sample using a Gilian Gilibrator2 (Sensidyne). Size selection was accomplished using MSP Model 200 Personal Environmental Monitors (PEM-10-2.5 and PEM-10-10) for $PM_{2.5}$ and PM_{10}, respectively. Filter samples were started just before the emission event and collected at least through the end of the source-generating activity and often until particle concentrations were close to pre-source levels (Table S1). Filters were equilibrated at a temperature of 19.5 ± 0.5°C and relative humidity of 47.5 ± 1.5% for at least 24 hours before weighing pre-and post-sampling on a Sartorius SE2-F ultra-microbalance.

A Grimm Mini Wide-Range Aerosol Spectrometer Model 1371 (WRAS) was used as a reference transfer for one minute resolved data and also to provide distributions of particle number and mass concentrations. The WRAS combines an electrical mobility analyzer that counts particles in 10 size bins from 10 to 193 nm with a laser-based optical particle counter that provides counts

in 15 bins from 0.25 to 2.5 μm and 16 bins from 2.5 to 35 μm. WRAS output was adjusted with source-specific factors determined using the filters and TEOM, as described in Section 2.7.

2.3. Professional grade particle monitors

Measurements were additionally made with two professional grade aerosol photometers: a Met One Instruments BT-645 (BT) and a Thermo pDR-1500 (PDR). These instruments have wide measurement ranges, from 1 μg m^{-3} to 100 and 400 mg m^{-3}, respectively. They use lasers with wavelengths of 670 and 880 nm, respectively, and have active flow control and filtered sheath air to keep their optical paths clean. The PDR features temperature and humidity compensation. The BT is calibrated with 0.54 μm polystyrene latex spheres and the PDR is calibrated with Arizona test dust (ISO 12103-1, A2 Fine). Manuals for both recommend that the instruments should be adjusted for specific sources or sampling environments by co-located gravimetric sampling. The PDR has an onboard filter slot.

2.4. Test room set up

All experiments occurred in a single-story 120 m^3 laboratory room with three external walls, two doors and raised ceiling. Particle monitors were placed on or adjacent to a wire shelving unit in the central area, several meters from source activities (Figure 1). Outdoor air was supplied to the chamber through a HEPA box air filter (McMaster-Carr 2153K49) at an air exchange rate of 1.4–1.5 h^{-1}. The rate was measured several times through the testing period by tracer decay. Small fans were operated to mix the air.

2.5. Source descriptions

Table 2 presents brief descriptions of the 24 source experiments. Several sources were used in multiple experiments, sometimes with variations. Sources are discussed in the following groups. Mineral sources included an ultrasonic humidifier with the filter removed, Arizona Test Dust, and vacuuming with the HEPA filter removed. Recreational combustion included candles burning and being extinguished (with separate filters collected for each phase), stick incense and mosquito coils. Electric cooking activities included microwaving popcorn, cooking of beef burgers on an electric grill (e-grilling), heating oil in a steel wok on an induction stove, and toasting 6 slices of

bread in a toaster. There were four cooking activities with pan-frying (bacon, eggs, fish) or stir-frying (spinach), all on gas burners. And there were four cooking experiments that did not involve frying or stir-frying: boiling potatoes on a gas stovetop and separately broiling Brussel sprouts, potatoes, and bacon in a gas oven.

To evaluate the performance of the low-cost devices at measuring indoor concentrations of infiltrated outdoor $PM_{2.5}$, data were also collected during two overnight periods during which the filtered ventilation air was turned off and the exterior door was partially opened to increase outdoor air exchange. We also analyzed data from overnight and weekend periods when the room was closed and the filtering of supply air resulted in very clean conditions; these data enable assessment of low-cost monitor response when $PM_{2.5}$ is close to zero.

2.6. Data recording and processing

For the AQE and AVP, we used on-board storage and downloaded data via computer-based software (AQE) or by connecting to the device via local Wi-Fi using the SAMBA protocol (AVP). Data from the AW2 devices were provided by the company in response to an email request to the product technical support center. Data from the LE2, PAI and IKA were obtained from online data storage platforms. The LCMs and TEOM synchronized their internal clocks to official time by internet connection. The WRAS clock was reset each day to the same computer, which was also synchronized to official time.

2.7. Data analysis

The general approach to estimating the true $PM_{2.5}$ time series during source activities was to use the gravimetric samples and the TEOM data to adjust the WRAS. Source-specific adjustments were determined by comparing average concentrations reported by the WRAS, TEOM and filters over the filter sampling intervals. Low-cost monitors were then compared to the adjusted WRAS for temporal correlation (at 5-min resolution) and for accuracy measuring event-integrated mass concentrations. The accuracy of LCMs for infiltrating outdoor PM and their readings when exposed to clean air (near-zero values) was evaluated by direct comparison to hourly TEOM data.

We screened for any filter-based data that appeared to be inconsistent with the co-located mass-based measurements (i.e. the other filter and TEOM). Filter-based $PM_{2.5}$ measurements were first compared to TEOM data collected over the same intervals. The two were highly correlated with r^2=0.94 and the filters higher than the TEOM by about 16% as a group (Figure S1 of the SM). None of the paired filter and TEOM $PM_{2.5}$ measurements differed by more than a factor of 2. The largest differences were for snuffed candles (0.51), dust (0.61), humidifier 1 (0.65) and boiled potatoes (1.46). The error for the potatoes is assumed to be related to the small mass collected on the filters (~5 mg).

We also compared $PM_{2.5}$ and PM_{10} filters. Since the WRAS robustly detects the particles that comprise the difference, we used the ratio of $PM_{2.5}$ to PM_{10} reported by the WRAS as an estimate of what the ratio should be. There were three events for which the ratio of $PM_{2.5}$ to PM_{10} determined by filter samples was more than a factor of 2 different than the ratio reported by the WRAS. Two of the events (on the same day, 14-Dec) appeared to have erroneous filter measurements. The PM_{10} filter for the second mosquito coil experiment indicated 262 μg m^{-3} whereas the $PM_{2.5}$ filter and TEOM had concentrations of 66.8 and 70.8 μg m^{-3}. Additionally, the WRAS indicated that $PM_{2.5}$ and PM_{10} should have been almost the same for the mosquito coil and the $PM_{2.5}$ and PM_{10} from filters were very close for the first coil experiment. For the Test Dust, the PM_{10} filter indicated a concentration of 74 μg m^{-3} while the $PM_{2.5}$ filter indicated 45 μg m^{-3}. Since the $PM_{2.5}$ filter sample translated to an aerosol density of 2.34 μg m^{-3}, which is close to the Test Dust density of 2.65 μg m^{-3}, we used the density adjustment factor from the $PM_{2.5}$ filter for both samples.

As a second data check we compared $PM_{2.5}$ and PM_{10} concentrations estimated from filters for all sources that the WRAS indicated had more than 95% of the PM_{10} mass under $PM_{2.5}$. If we include the filters collected during the period when the room was opened to the outdoors to measure ambient air overnight on 12/20-12/21 there were 14 events that fit this criterion. We calculated the ratio of $PM_{2.5}$ to PM_{10} based on WRAS and also based on the filter samples. The WRAS ratio for this group was 0.974+/-0.016. The ratio of gravimetric samples was 0.912±0.089.

This suggests a possible systematic bias of roughly 6-7% between the pumps and PEMs used to sample $PM_{2.5}$ and PM_{10}. The relative standard deviation of four filter samples from the humidifier experiment (which had true duplicates for both $PM_{2.5}$ and PM_{10}) was 14%. The relative deviations for the other 13 pairs of $PM_{2.5}$ and PM_{10} samples had a mean of 0.118 and SD of 0.057. In all subsequent analyses, we used the average of the $PM_{2.5}$ and PM_{10} gravimetric concentrations for these 14 events.

The best estimates of actual $PM_{2.5}$ concentrations developed from the analysis described above were used to adjust the WRAS data for each source. These factors are presented as density adjustment factors (DAF) in Table 1. WRAS data were multiplied by DAF/1.68 as 1.68 is the default density assumed in the WRAS.

Low-cost monitor data were visually reviewed to screen for any clearly questionable data. This simple quality assurance check found that one of the AQE units occasionally reported elevated concentrations when there were no sources indicated by the other two (see Figure S2).

2.8. Temporal correlations

To assess temporal correlation for emission events, we compared data pairs of $PM_{2.5}$ reported by each low-cost monitor and the adjusted WRAS concentrations averaged over the same 5 min intervals. An event analysis interval was set for each experiment by visually inspecting the time series data to ensure that the entire period of elevated concentration was included (from just before the start of an event until after the room has decayed to pre-event levels). Low-cost monitor data were regressed against the adjusted WRAS for each source using a linear model with zero intercept, a linear model with floating intercept, and a second order polynomial with floating intercept, and the R^2 was calculated for each fit.

2.9. Calculation of time-integrated concentration by source event

Performance for measuring events was assessed as a monitor's ability to accurately report the time-integrated concentration over the event. Events were quantified by subtracting the baseline room air concentration before and after the event. For each device, the baseline was identified by first masking all data points >2 $\mu g\ m^{-3}$ above the concentrations measured at the start and end of

the interval. This baseline was then subtracted from each data point in the interval and baseline-subtracted concentrations were integrated over time. Ratios of device response to adjusted WRAS (estimated true PM) were calculated for both baseline-subtracted and as-reported data series.

3. Results

3.1. Low-cost monitor response for clean air and infiltrated outdoor $PM_{2.5}$

A common starting point for assessing instrument performance is to check the output when the target analyte is absent, i.e. to check the zero. Since this study sought to assess performance for realistic challenges, we conducted a near-zero check while there were no sources inside the room and the supply air was effectively filtered. The hourly $PM_{2.5}$ concentrations measured by the TEOM during these periods, show in Figure 2 and Figure S5 had a mean ± standard deviation (SD) of 1.45±2.0 μg m^{-3}. This SD matches the manufacturer specified precision of ±2 μg m^{-3} for hourly data. At these conditions all low-cost monitors frequently or mostly reported hourly $PM_{2.5}$ under 0.5 μg m^{-3} and several (AVP, IKA, AQE, LE2) commonly reported $PM_{2.5}$ under 0.1 μg m^{-3} (Figure S5). These results indicate a small negative offset for the low-cost monitors, corresponding to under reporting at very low concentrations.

Figure 2 also presents the hourly $PM_{2.5}$ measurements from LCMs and the TEOM during the overnight periods with the exterior door slightly open to increase outdoor air infiltration and the filtered supply turned off. Hourly $PM_{2.5}$ as measured by the TEOM was very low during the first night and reached approximately 15 μg m^{-3} during the second night. The LCMs tracked the TEOM with linear-fit R^2 values of 0.75–0.80. The variance resulted primarily from the LCMs but imprecision in the hourly TEOM was also a factor at these low levels. The best fit lines had negative offsets of 2-5 μg m^{-3} (Table S2), again indicating under-reporting near zero. Figure 2 also show that for infiltrated outdoor $PM_{2.5}$, devices with Plantower sensors (AQE, LE2, and PAI in bottom row) had higher slopes than devices using other sensors (Table S2). Comparisons of the TEOM to the unadjusted WRAS and the professional PM monitors are provided in Figure S6. Similar to the low-cost monitors, both professional grade devices had negative offsets around

3 μg m^{-3} and slopes of 1.4 and 2.0. The unadjusted WRAS was much closer to the TEOM with a slope of 1.2 and a positive intercept of 0.3 μg m^{-3}.

3.2. Temporal correlations to estimated true $PM_{2.5}$

Correlations between 5-minute average $PM_{2.5}$ reported by LCMs or professional photometers and the coincident adjusted WRAS (reference) measurements are presented for all of the PM sources in Figures S7-S18 of the Supplementary Material. Example LCM results for 8 sources are provided in Figures 3–4. At the top of each column is the mass distribution by particle size, obtained by applying the density adjustment factors in Table 2 uniformly across the size distribution reported by the WRAS. As a visual aid, the $PM_{2.5}$ contributed by particles in the optical range of the WRAS (starting at 0.25 μm optical diameter) are colored green and smaller particles – which should be invisible to the optical sensors of the LCMs – are displayed in red. Yellow shading is used to indicate mass contributed by coarse particles, between 2.5 and 10 μm diameter. For most of the LCMs, there are three points at each time step, one for each unit tested. The AQE that intermittently reported spurious readings was removed leaving only two units for that device. Variance across units of a device is visible as vertical separation of data points. Asterisks indicate measurements when concentrations were rising and open circles show decays. Parameters of linear or second order fits are shown.

All monitors had substantial responses to the three mineral sources, as shown in Figures S7–S8 and the first two columns of Figure 4, with generally higher response to the unfiltered ultrasonic humidifier aerosol than for the unfiltered vacuuming or Test Dust. This corresponds to the humidifier having a much larger fraction of mass in the optical sensing range for $PM_{2.5}$. The AVP and AW2 had the most consistent response across the three sources, providing among the highest responses for vacuuming and dust, but somewhat lower responses compared to other monitors for the humidifier aerosol. For these three sources, the largest variation in responses across devices occurred for the Test Dust, for which the $PM_{2.5}$ mass was almost entirely at the upper end of the size range. Low-cost monitor responses were highly correlated to the reference with $R^2 \geq 0.83$ in all

cases. Similar to LCM responses, professional monitor slopes were higher for the humidifier (0.8–1.2) than for the vacuum and Test Dust (0.4–0.5) (Figure S8).

Figures S9–S10 presents results for replicate experiments with incense and mosquito coil. These sources had similar mass distributions by size, roughly split between particles above and below the threshold for optical detection. Each monitor had similar responses for the two sources and consistent responses for replicates. All showed high linear correlation with $R^2 \geq 0.98$. Slopes were substantially above unity, indicating over-reporting of $PM_{2.5}$.

LCM responses to unscented candle burning and snuff phases are shown in Figure 4 and results for both candle experiments are provided in Figures S11-S12. During the burn phase for unscented candles, the WRAS indicated very little mass in the nominally visible range of the optical sensors, yet both the LCMs and professional monitors tracked the adjusted WRAS with high linear correlations ($R^2 \geq 0.95$). Slopes varied from 0.25 for the AVP to 0.76 and 0.78 for the PAI and AQE, suggesting that sensors may be variably weighting the signal from the smallest particles that they can detect. After the unscented candles were snuffed, mass concentrations increased and a larger fraction was in the detectable range of the optical sensors; consequently, concentrations reported by the LCMs were closer to the estimated true $PM_{2.5}$ (slopes closer to 1). Correlations were a bit lower for this phase of the experiment owing to somewhat different responses during the very short period of increasing concentrations (asterisks). During steady burning of the scented candles, the adjusted WRAS indicated concentrations rising to about 25 μg m^{-3} but no LCM response, as all of the mass presented in particles smaller than 0.2 μm. After the scented candles were snuffed, many larger particles were formed and the mass concentrations in the $PM_{2.5}$ and coarse (PM_{10}–$PM_{2.5}$) ranges were of similar magnitude to the mass concentration of particles below 0.25 μm. Most of the LCMs again had initially low response (indicated by the asterisk data points shown below the main correlation lines in Figure S11) and higher responses during the decay. Figure S12 shows that the professional monitors had similar responses to the LCMs for candles; they reported no substantial $PM_{2.5}$ during the scented candle burning phase and reported

$PM_{2.5}$ that was half or less of the estimated true value during the continuous burn of the unscented candles. Professional monitors also under-reported $PM_{2.5}$ after candles were extinguished.

Results from the electric grilling of a burger and heating olive oil on an induction stove are presented in Figure 4 and full results for the electric cooking group are provided in Figure S13–S14. All of the monitors had high correlations to the adjusted WRAS for all of the electric cooking events, though the response factors varied. The toast produced the lowest response and the olive oil had the highest for most monitors. Slopes were also high for e-grilled beef burgers, which had substantial mass in particles >0.25 μm. The very high response factors for the induction-heated olive oil were somewhat surprising since only a small faction of its mass was in the particle size range thought to be visible by the optical sensors. These results sharpen the question of how the sensors are estimating mass for the smallest detected particles. Similar to the LCMs, the professional monitors were highly correlated for all sources but with varying slopes (Figure S13).

The third column of Figure 4 presents broiled bacon as an example of cooking with gas burners without frying, and results from other sources in this group are presented in Figures S15–S16. For these sources, $PM_{2.5}$ was comprised entirely or almost entirely of particles smaller than 0.25 μm and based on the data, invisible to the optical sensors of both the low-cost and professional monitors. None of the monitors reported any significant mass despite the adjusted WRAS reporting 5-min average concentrations exceeding 30, 50, 100, and 100 μg m^{-3} for the four events.

Figures S17–S18 presents results for the four events with cooking involving frying or stir-frying and the frying of bacon is shown as an example in Figure 4. For these sources, roughly half or more of the $PM_{2.5}$ was in the optical detection range of the WRAS. All of the LCMs and professional monitors were highly correlated to the adjusted WRAS for all four sources, with slopes varying from approximately 0.5 to 1.5. For these sources, the responses across LCMs for each source varied less than for any of the other source groups. We note, however, that each LCM had different response to the specific frying or stir-frying sources. It is also notable that several of the LCMs had a non-linear response at the very high $PM_{2.5}$ produced by the bacon frying; these were fit with a second order polynomial as shown in Figure 4.

The correlation analysis revealed the following points. When there was substantial mass in particles above 0.25 μm, all LCM $PM_{2.5}$ concentrations were linearly correlated with the estimated true $PM_{2.5,}$ at least up to 200 μg m^{-3}; and slopes were almost always in the range of 0.5–2.0. When the $PM_{2.5}$ was entirely comprised of particles smaller than 0.25 μm optical diameter, invisible to the optical sensors of both the low-cost and professional monitors, none reported significant events. Relatively high LCM responses for sources with little mass in the optically invisible range raise questions about how the sensors weight the signal from the smallest particles.

3.3. Accuracy for quantifying event-integrated $PM_{2.5}$

In the following sections, we compare as-measured and baseline-subtracted, event-integrated concentrations reported by LCMs to those from adjusted WRAS data. We used the adjusted WRAS as the reference because it provided data resolved to 1 minute with no apparent delay. Figure 5 and Figure 6 present results as ratios of the event-integrated values for the 24 sources described in Table 2. Open circles show ratios calculated using baseline-subtracted concentrations, x-symbols indicate the as-measured ratios. Error bars indicate the standard deviations of the ratios developed from the 2–3 units of each monitor. The pie chart in each panel shows the estimated size-resolved mass distribution provided by the WRAS, with the same color codes used previously. The overall size of the pie is proportional to the integrated mass over each event.

Figure 5 presents results for mineral and combustion sources. With the exception of the burn periods of scented candles – for which all LCMs had little response – the LCMs generally reported event-integrated concentrations within a factor of 2 of the estimated true $PM_{2.5}$ for all sources in these categories. Relative responses of the LCMs were similar for the vacuum and Test Dust, for the stick incense and mosquito coil sources, for the two humidifier experiments, and for the two parts of the unscented candle source; but the patterns were different across these source groups.

Figure 6 presents the event-integrated $PM_{2.5}$ comparison for varied cooking activities. All the LCMs missed the boiled potatoes and broiled bacon, potatoes, and Brussels sprouts. Ratios of baseline subtracted integrations were also near zero for the toast; the as-measured values were substantially higher if still small overall. The responses across LCMs varied the least for popcorn;

e-grilling of a beef burger; stir-frying spinach; and pan-frying eggs, bacon or fish. The highest response factors and largest variations across LCMs occurred for oil heating. Pan-fried fish had a different response pattern than pan-fried bacon and eggs, due to different particle size distribution.

Overall, the event-integrated analysis provides findings that are consistent with those of the correlation analysis. All of the LCMs provided at least semi-quantitative responses (roughly within a factor of 2) to most of the sources, but all missed small to medium sized sources comprised entirely of particles smaller than about 0.25 μm optical diameter.

3.4. Accuracy for quantifying event-integrated PM_{10}

Figures 7–8 present the event-integrated PM_{10} and $PM_{2.5}$ concentrations for the low-cost monitors that report both parameters and also presents the same results for the adjusted WRAS. These results have several features that are relevant to the interpretation of PM_{10} reported by LCMs. The first finding is that one of the three AVP units reported much higher PM_{10} than the other two units in 13 of the 24 experiments. The AVP and the AQE commonly reported substantially higher PM_{10} than $PM_{2.5}$ when the adjusted WRAS indicated similar concentrations for the two PM size cuts. The AQE, AVP and PAI all reported varied, non-zero PM_{10} for the boiled potatoes, and broiled Brussels sprouts, bacon and potatoes, even though these sources appeared to have almost no coarse mode particles based on the adjusted WRAS. There were several sources for which an LCM reported PM_{10} that was similar to the adjusted WRAS but much higher than the $PM_{2.5}$ reported by the LCM for the same source, even though the WRAS indicated no substantial coarse mode mass; examples include the post-snuff phases of candles, toast, and e-grilled burner. Overall, these results indicate that the PM_{10} data from the low-cost monitors may be less consistent and reliable than the reported $PM_{2.5}$.

4. Discussion

All of the LCMs tested in this study reported $PM_{2.5}$ within a factor of two of the estimated true mass concentrations for most of the sources evaluated. This was an improvement on the performance of home IAQ monitors as a group compared to our prior study[22]. The aerosols that

were effectively measured varied in size distribution and chemical composition; but all had at least some mass in the optical sensing range of the research-grade WRAS monitor. There were some sources for which the $PM_{2.5}$ reported by an LCM was higher than the *total* $PM_{2.5}$ mass estimated from the adjusted WRAS even though much of the mass reported by the WRAS for that source was contributed by particles smaller than the optical size detection range; this is another indicator of the sensors in the LCMs over-weighting the smallest particles that they detect. In contrast, most of the LCMs reported concentrations that were less than half of the estimated actual $PM_{2.5}$ emitted from vacuuming and Test Dust, for which most of the $PM_{2.5}$ was in particles larger than 1 μm.

The LCMs missed the $PM_{2.5}$ emitted from the steady burning of candles and electric or gas cooking that did not involve frying, stir-frying or heating of oil. While this shows that these devices still have limitations, it is important to recognize that professional monitors that rely on optical sensing have similar blind spots.

The variability of LCM response factors by source complicates their use for quantitative assessment of indoor concentrations and exposures. Professional grade monitors have this same limitation and require gravimetric sampling for environment or source-specific calibration factors. LCMs may nevertheless provide effective event detection and accurate if imprecise estimates of the benefits of instituting controls or interventions if the mix of sources (and thus response factors) is similar before and after the intervention. Research is needed to assess that possibility.

Although three LCMs (AQE, LE2, and PAI) used Plantower sensors with the same nominal performance specifications, the integrated $PM_{2.5}$ mass concentrations reported by these devices differed substantially for some sources. The AQE and PAI reported moderately different (relative deviation of >10%) integrated $PM_{2.5}$ for incense, mosquito coils, burning candles, pan-frying bacon, and stir-frying spinach. The LE2 reported significantly lower integrated mass than the AQE and PAI for the humidifier operating without filter, test dust, vacuum, and cooking involving frying. It is not known if the differences resulted from a different measurement configuration across versions of the Plantower sensor or an adjustment of the sensor signal by the LE2.

There was generally high consistency across the three units of each model tested in this study. Among the 18 units tested, we identified only one with a faulty sensor that impacted results. This was easily identified by co-locating multiple units of a single device or could also be detected by comparison to other LCMs. This is a check that home users could do by comparing multiple devices in the presence of sources. When the unit with the bad sensor was excluded, the relative standard deviations for all LCMs across most events was less than 5%. The exceptions were the events in which much or all of the $PM_{2.5}$ presented in particles <0.25 μm or >1 μm. The PAI units had the highest standard deviations, exceeding 8% in the cooking activities.

We note as a limitation that this study did not evaluate the effect of temperature or humidity on LCM performance. Product specifications provided by the sensor manufacturers indicate that the effect of temperature is negligible in the range of 10-40 ℃, but high humidity is known to affect aerosol optical sensing and could be relevant in some residential applications.

5. Conclusions

Six low-cost IAQ monitors were evaluated for their responsiveness and accuracy in measuring $PM_{2.5}$ and PM_{10} generated by common residential sources. All of the LCMs had semi-quantitative responses (within a factor of two) to most of the sources but all had very little or no response when the generated aerosols were entirely or almost entirely below the optical threshold of roughly 0.25 μm. With the exception of one monitor with a faulty sensor – which was easily identified using simple quality assurance data review - there was close agreement across three unit of each monitor for all the sources with substantial PM in the visible range of the optical sensors.

Table 1. Descriptions of Low-Cost Monitors

Device; Cost[1]	Data[2]	Particle sensor(s) and specifications for $PM_{2.5}$	Website for product information. Calibration and quality assurance information provided by manufacturer
Air Quality Egg 2018 version (AQE); US$225	1 min	Two Plantower PMS5003 [3] Effective range: 0–500 μg/m^3 Max. range: ≥1000 μg/m^3 Max. consistency error: 0~100 μg/m^3: ±10 μg/m^3 100~500 μg/m^3: ±10%	https://airqualityegg.com/home *Device reports $PM_{2.5}$ and PM_{10} as averages of concentrations reported by the two sensors. Each device is checked for consistency with other devices before shipping by exposure to incense smoke in a small room.*
IQAir AirVisual Pro (AVP); US$269	10 sec	AirVisual AVPM25b Effective range: 0–1798 μg/m^3	https://www.airvisual.com/ *Sensors calibrated through automatic process in controlled chamber, using distinct aerosols for PM_1, $PM_{2.5}$, PM_{10} using Grimm 11-A as reference. Firmware onboard diagnostic detects faults and reports to company server; customers contacted.*
Awair 2nd Edition (AW2); US$199	10 sec	Honeywell HPMA115S0 Accuracy @25±5ºC: 0–100 μg/m^3: ±15 μg/m^3 100–1000 μg/m^3: ±15%	https://getawair.com/products/awair-2nd-edition. *Provides $PM_{2.5}$ and estimated PM_{10} (μg/m^3) direct from sensor. Each device is checked for consistency with other devices and a reference sensor before shipping. Sensor rated for 5-7 y of continuous use. No recalibration or cleaning needed if used in typical indoor environments (e.g. office, residential, school).*
Kaiterra Laser Egg 2 (LE2); US$169	1 min	Plantower PMS3003 Same specification as PMS5003	https://www.kaiterra.com/en/laser-egg/ *If device configured with location, Kaiterra adjusts sensor output based on local outdoor PM (details proprietary); otherwise uses proprietary default calibration. Monitors tested in batches with varied sources including wood smoke and cigarette smoke.*
PurpleAir Indoor (PAI); US$179	80 sec	Plantower PMS1003 Same specification as PMS5003	https://www.purpleair.com/sensors *Provides data direct from sensor: PM_1, $PM_{2.5}$ and PM_{10} in μg/m^3, number concentrations (#/0.1L) of particles larger than the following optical diameters: 0.3, 0.5, 1.0, 2.5, 5.0, 10 μm.*
Ikair (IKA); ~US$150	1 min	TGF PM D4 Range: 0-1000 μg/m^3; Accuracy: 0–100 μg/m^3: ±10 μg/m^3 100–1000 μg/m^3: ±10%	http://www.tgftech.com/ *Provides $PM_{2.5}$ (μg/m^3) direct from sensor.*

[1] In October 2018. [2] Highest time resolution available. [3] Plantower documentation describes the analytical method as follows: "…collect scattering light in certain angle [and] obtain the curve of scattering light change with time. [By microprocessor, calculate] equivalent particle diameter and the number of particles with different diameter per unit volume based on MIE theory. Product documentation also reports "endurance max error" after 720 hours of operation: as ±15 μg/m^3 for 0~100 μg/m^3 and ±15% for 100~500 μg/m^3.

Table 2. Summary description of source activities

Source	Day[1]	Start time	Description	Peak $PM_{2.5}$ [2] μg m^{-3}	Peak PN[3] >10 nm, cm^{-3}	Est. $PM_{2.5}$ density [4]
Humidifier 1	10	10:24	Ultrasonic humidifier, cleaning cartridge removed; operated ~30 min	79	1.8×10^4	2.16
Humidifier 2	10	13:00	Ultrasonic humidifier, cleaning cartridge removed; operated ~90 min	119	2.4×10^4	2.22
Microwave popcorn	11	14:00	90 g popcorn (Newman's Own), heated in microwave 90 s	81	2.1×10^4	1.32
Incense stick 1	11	13:12	2 incense sticks (Shanthimalai Red Nag Champa) burned ~15 min	202	7.3×10^4	1.16
Toast white bread	12	9:12	6 slices of white bread, medium-toasted in used, 2-slice toaster	57	1.3×10^5	0.67
E-grilled burger	12	12:12	4 beef burgers (113 g each), cooked for 10 min on electric burger grill	126	1.5×10^5	0.89
Mosquito coil 1	12	15:06	Mosquito coil (Patio & Deck) burned for 15 min	125	1.1×10^3	1.18
Boiled potatoes	13	8:06	937g potatoes, peeled and cut; boiled for 25 min on gas stove	36	7.2×10^4	0.88
Unscented candles	13	11:36	6 unscented candles, lit with butane lighter, burn 54 min	102	9.2×10^4	1.05
Snuff candles	13	12:36	Extinguished candles and traced decay	163	9.7×10^4	1.03
Scented candles	13	15:54	3 scented candles, 3 wicks each, lit with butane lighter, burn 53 min	27	4.0×10^4	1.21
Snuff candles	13	16:54	Extinguished candles and tracked decay	54	4.5×10^4	1.52
Broil Br. sprouts	14	7:54	454 g brussels sprouts, broiled in oven at 204 ℃ for 20min	72	2.3×10^5	0.63
Arizona test dust	14	11:36	Arizona Test Dust (0-3μm) manually puffed from plastic blower	134	1.2×10^3	2.37
Stir-fry spinach	14	14:06	360 g spinach + 15 g canola oil, stir-fried in steel wok on gas burner	276	8.3×10^4	1.35
Mosquito coil 2	14	17:00	Mosquito coil (Patio & Deck) burned for 15 min	131	4.4×10^4	1.17
Heat olive oil	17	8:00	15 g olive oil brought to bubble in steel wok on induction stove	99	4.8×10^4	0.88
Vacuum	17	11:36	Vacuum with HEPA filter removed, operated for 15 min	224	3.0×10^3	2.89
Pan-fry eggs	17	14:12	4 eggs, fully cooked with 15 g canola oil on gas stove	249	1.2×10^5	1.19
Pan-fry bacon	18	17:00	3 strips uncured apple smoked bacon, pan-fried on gas stove for 10 min	843	3.8×10^5	1.20
Pan-fry fish	18	7:48	320 g Tilapia fillets, pan-fried with 15 g butter on gas stove	84	1.1×10^5	0.91
Broil bacon	18	10:54	3 strips uncured apple smoked bacon, broiled at 218 ℃ for 14 min	110	3.6×10^5	0.63
Incense stick 2	18	13:30	Incense stick (Shanthimalai Red Nag Champa); burned for ~60 min	378	6.9×10^4	1.65
Broil potatoes	19	16:12	940 g peeled potatoes coated with 20 g olive oil; broiled at 218 ℃ 25 min	115	2.5×10^5	0.64

[1] Dec 2018. [2] Peak 1-min $PM_{2.5}$, adjusted WRAS. [3] Peak number conc. [4] Estimated from WRAS adjustment and default of 1.68 g/cm^3.

Figures

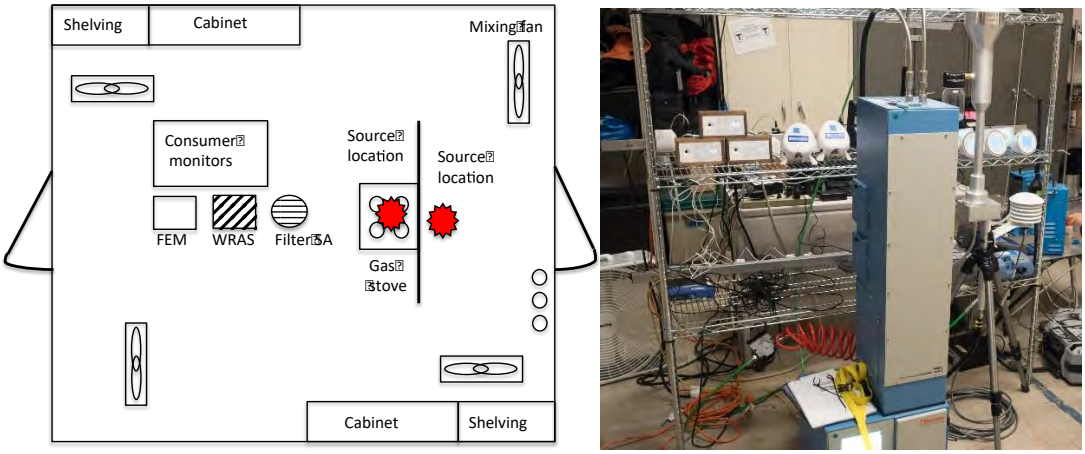


Figure 1. (a) Schematic of test room; (b) Photo of test set-up

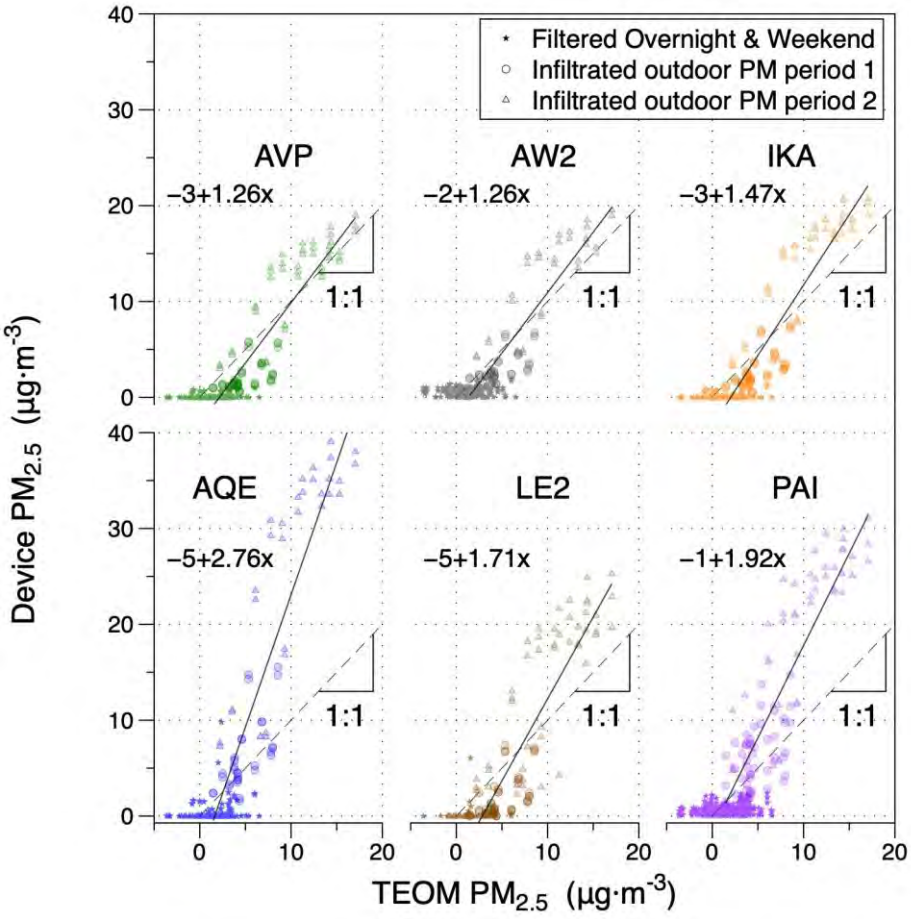


Figure 2. Hourly $PM_{2.5}$ reported by low-cost monitors and the TEOM during overnight periods with the room open to outdoor air and no filtration and during no-source periods with filtered supply air.

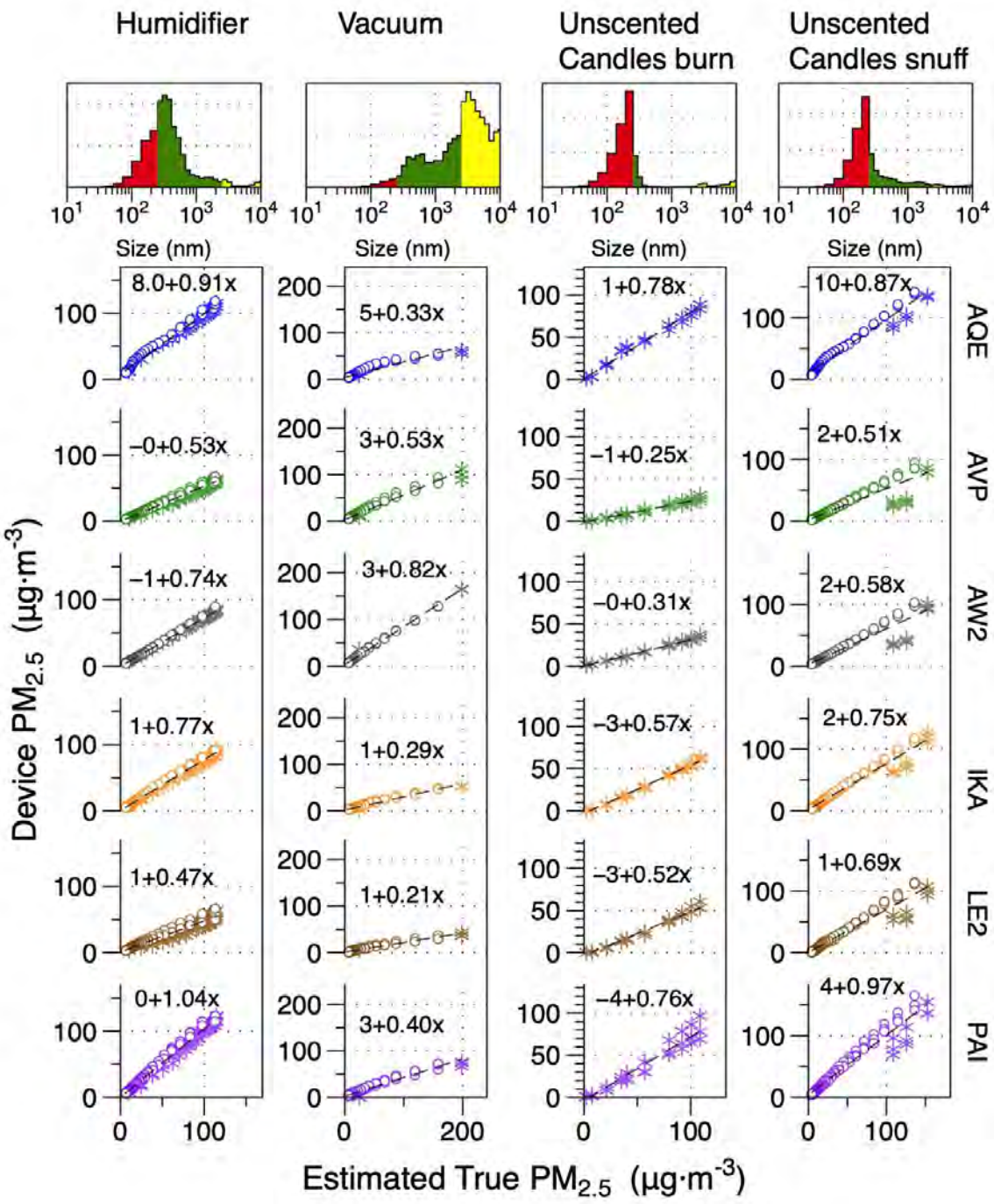


Figure 3. Correlations between 5-min average $PM_{2.5}$ reported by low-cost monitors and estimated true $PM_{2.5}$ from WRAS adjusted to gravimetric data for example mineral and combustion sources. Histograms at top show the distribution of PM mass over range of 10 nm to 10 µm. Additional results for these source groups and for professional monitors are in Supplementary Material.

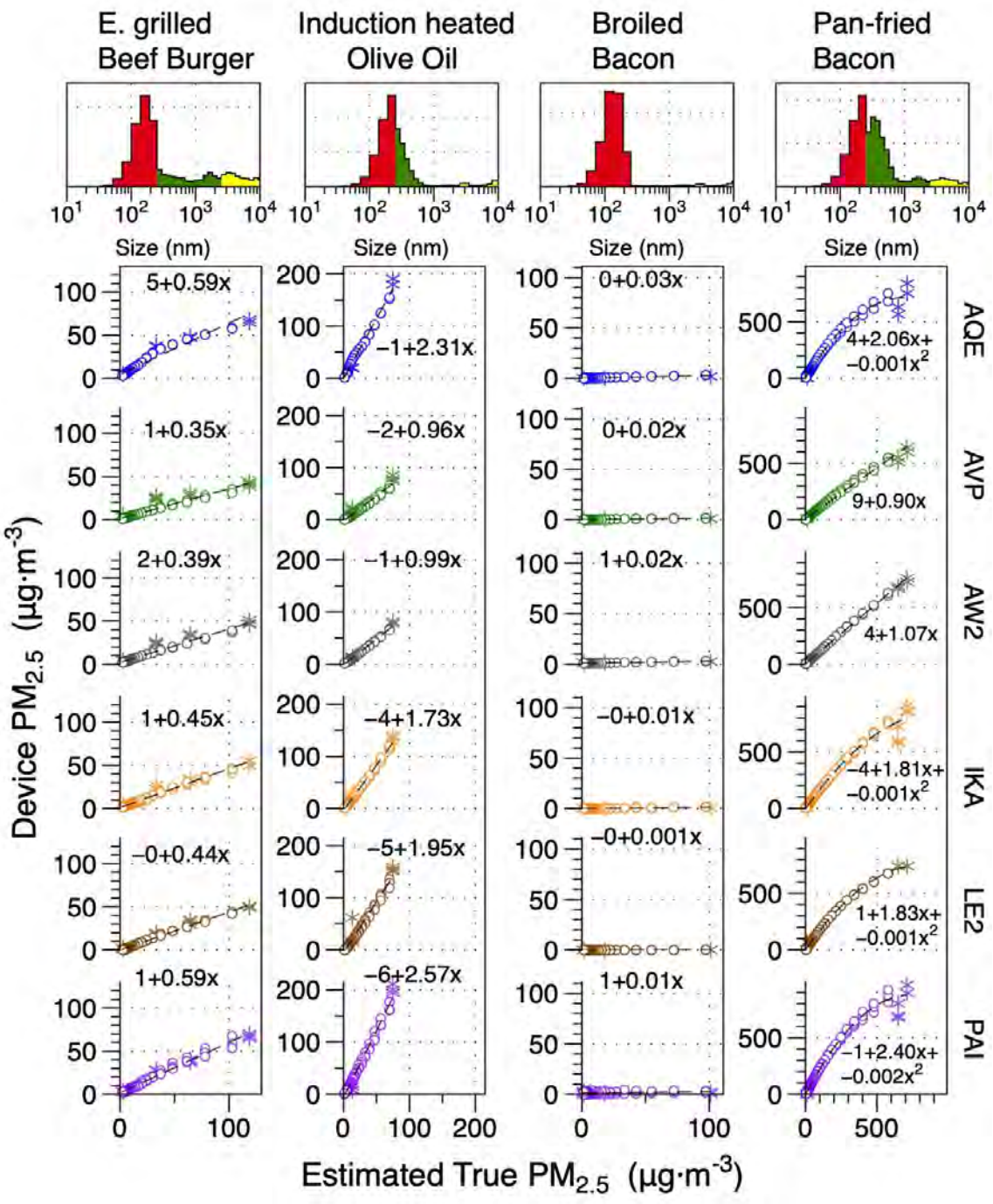


Figure 4. Correlations between 5-min average $PM_{2.5}$ reported by low-cost monitors and estimated true $PM_{2.5}$ from WRAS adjusted to gravimetric data for example cooking sources. Histograms at top show the distribution of PM mass over range of 10 nm to 10 µm. Additional results for varied types of cooking and for professional monitors are in Supplementary Material.

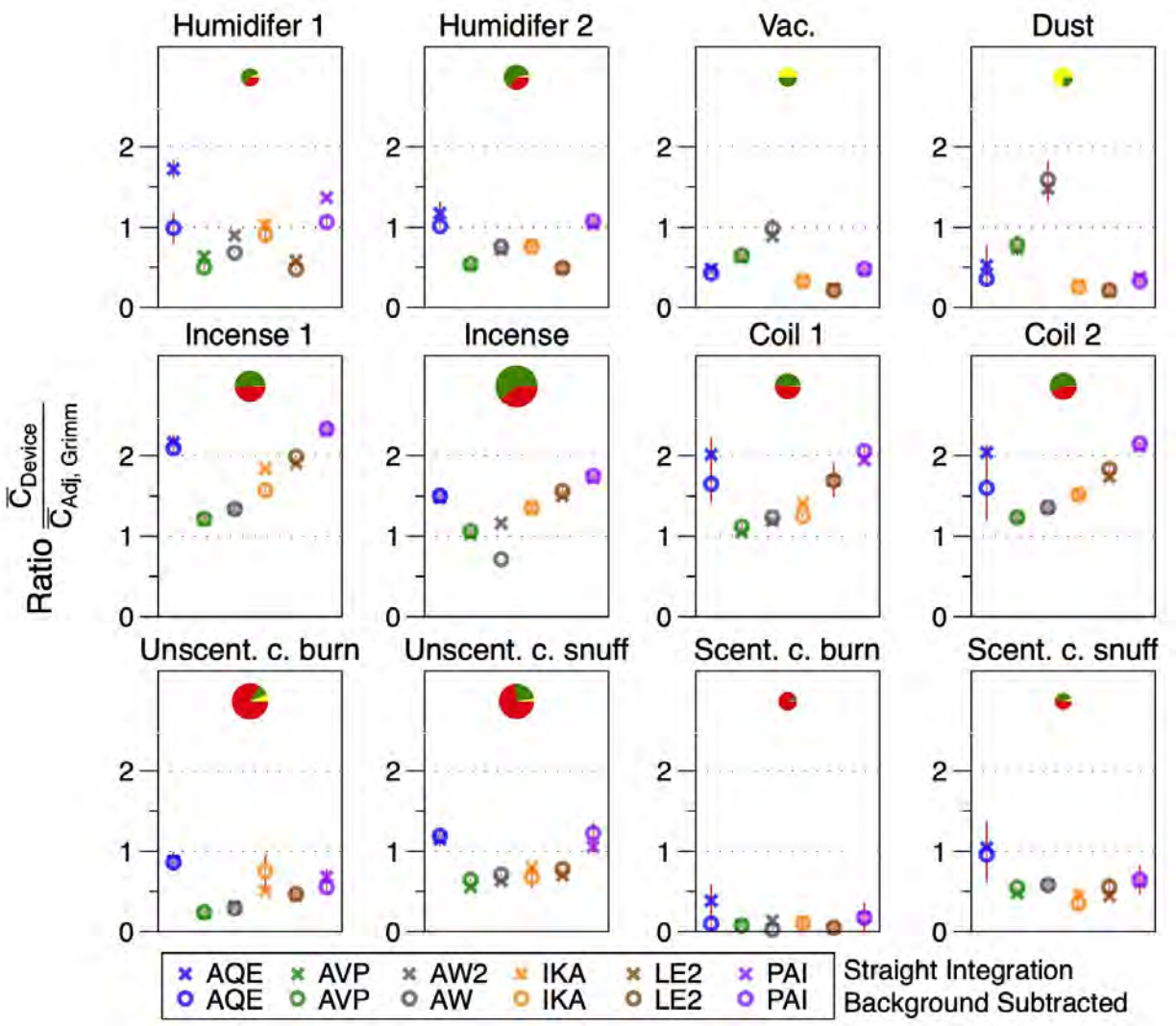


Figure 5. Ratios of event-integrated $PM_{2.5}$ reported by each low-cost monitor to the estimated true event-integrated $PM_{2.5}$ from WRAS adjusted by gravimetric data: mineral and combustion sources. Pie charts are sized proportionally to the estimated true PM_{10} integrated over the event with red, green and yellow corresponding to mass fractions of the following particle size ranges (in μm): 10–2.5, 2.5–0.25, <0.25.

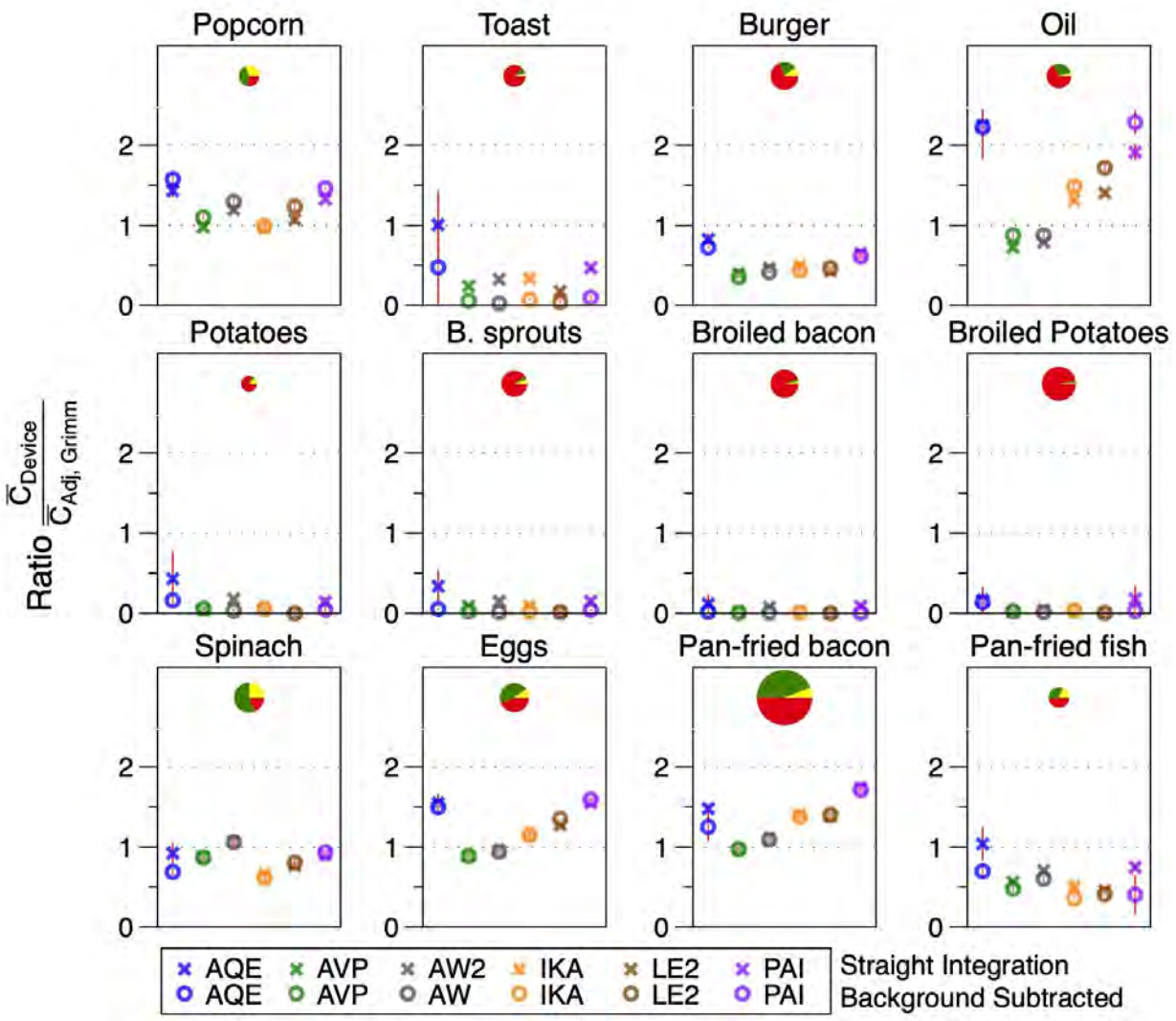


Figure 6. Ratios of event-integrated $PM_{2.5}$ reported by each low-cost monitor to the estimated true event-integrated $PM_{2.5}$ from WRAS adjusted by gravimetric data: cooking sources. Refer to Figure 5 caption for description of pie charts.

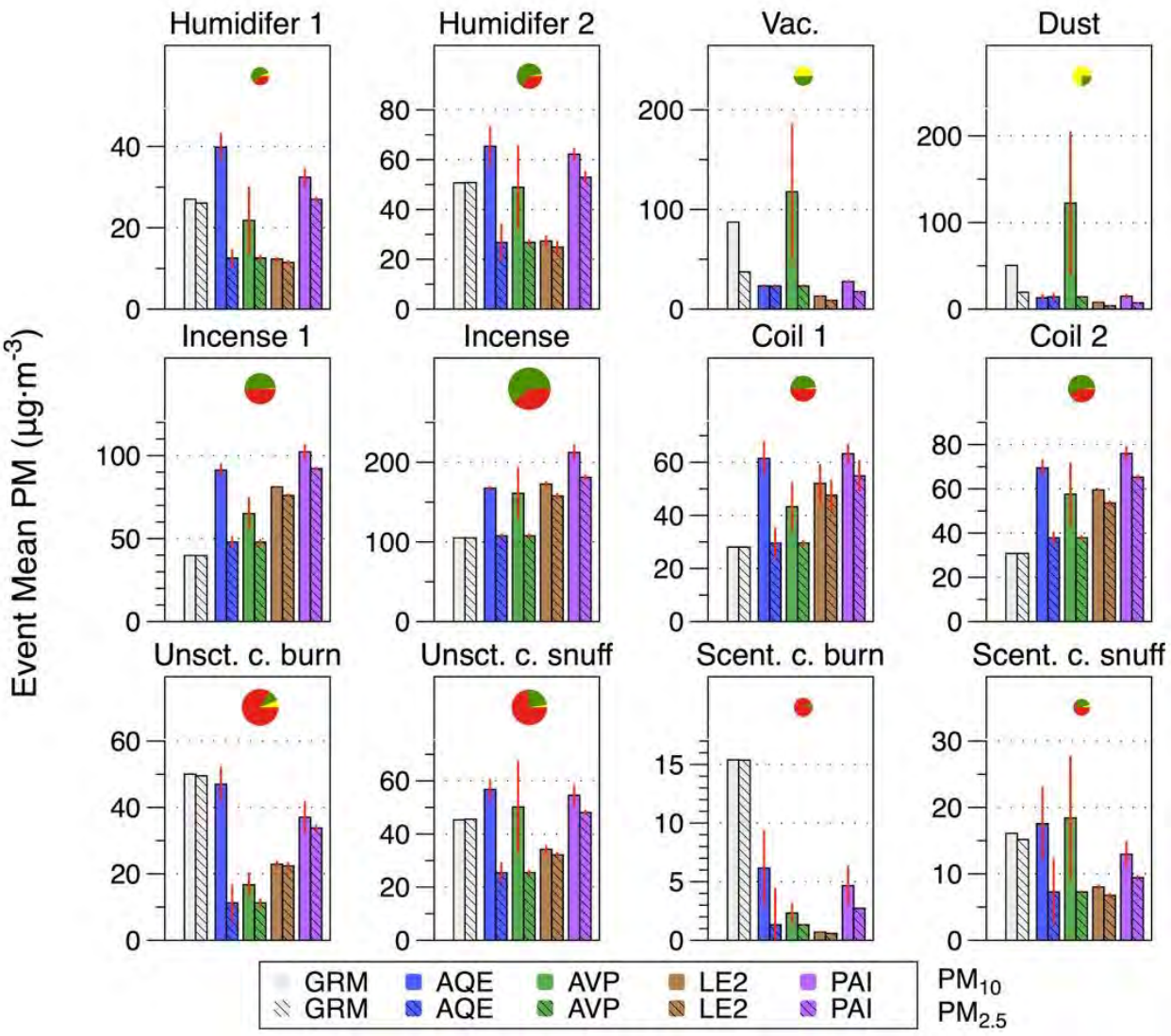


Figure 7. Event-integrated PM_{10} and $PM_{2.5}$ reported by each low-cost monitor and for the estimated true PM_{10} and $PM_{2.5}$ from WRAS adjusted by gravimetric data: mineral and combustion sources. Refer to Figure 5 caption for description of pie charts.

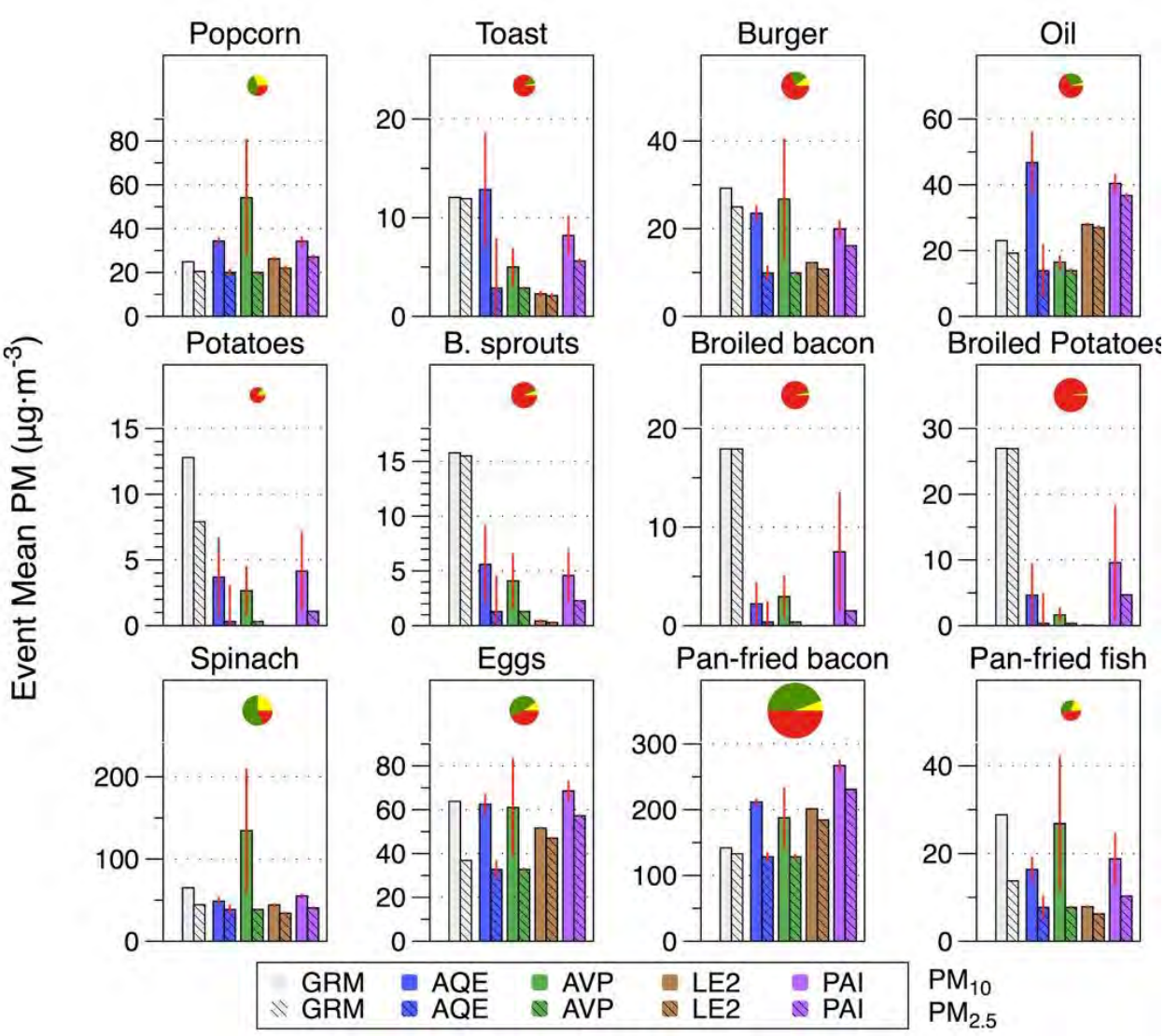


Figure 8. Event-integrated PM_{10} and $PM_{2.5}$ reported by each low-cost monitor and for the estimated true PM_{10} and $PM_{2.5}$ from WRAS adjusted by gravimetric data: cooking sources. Refer to Figure 5 caption for description of pie charts.

References

1. US EPA. *Final Report: Integrated Science Assessment for Particulate Matter*. Washington, DC: U.S. Environmental Protection Agency; 2009.
2. Abt E, Suh HH, Allen G, Koutrakis P. Characterization of indoor particle sources: A study conducted in the metropolitan Boston area. *Environ Health Perspect.* 2000;108:35-44.
3. Dobson R, Semple S. "How do you know those particles are from cigarettes?": An algorithm to help differentiate second-hand tobacco smoke from background sources of household fine particulate matter. *Environ Res.* 2018;166:344-347.
4. Min KT, Lundrigan P, Sward K, Collingwood SC, Patwari N. Smart home air filtering system: A randomized controlled trial for performance evaluation. *Smart Health.* 2018;9-10:62-75.
5. Schieweck A, Uhde E, Salthammer T, Salthammer LC, Morawska L, Mazaheri M, Kumar P. Smart homes and the control of indoor air quality. *Renewable & Sustainable Energy Reviews.* 2018;94:705-718.
6. Moore J, Goffin P, Meyer M, Lundrigan P, Patwari N, Sward K, Wiese J. Managing In-home Environments through Sensing, Annotating, and Visualizing Air Quality Data. *Proc. ACM Interact. Mob. Wearable Ubiquitous Technol.* 2018;2:1-28.
7. Chow JC. Measurement Methods to Determine Compliance with Ambient Air-Quality Standards for Suspended Particles. *J Air Waste Manag Assoc.* 1995;45:320-382.
8. Noble CA, Vanderpool RW, Peters TM, McElroy FF, Gemmill DB, Wiener RW. Federal reference and equivalent methods for measuring fine particulate matter. *Aerosol Sci Technol.* 2001;34:457-464.
9. Wang XL, Chancellor G, Evenstad J, Farnsworth JE, Hase A, Olson GM, Sreenath A, Agarwal JK. A Novel Optical Instrument for Estimating Size Segregated Aerosol Mass Concentration in Real Time. *Aerosol Sci Technol.* 2009;43:939-950.
10. Thomas A, Gebhart J. Correlations between Gravimetry and Light-Scattering Photometry for Atmospheric Aerosols. *Atmos Environ.* 1994;28:935-938.
11. MacNeill M, Kearney J, Wallace L, Gibson M, Heroux ME, Kuchta J, Guernsey JR, Wheeler AJ. Quantifying the contribution of ambient and indoor-generated fine particles to indoor air in residential environments. *Indoor Air.* 2014;24:362-375.
12. Kearney J, Wallace L, MacNeill M, Heroux ME, Kindzierski W, Wheeler A. Residential infiltration of fine and ultrafine particles in Edmonton. *Atmos Environ.* 2014;94:793-805.
13. Wallace LA, Wheeler AJ, Kearney J, Van Ryswyk K, You HY, Kulka RH, Rasmussen PE, Brook JR, Xu XH. Validation of continuous particle monitors for personal, indoor, and outdoor exposures. *J Exposure Sci Environ Epidemiol.* 2011;21:49-64.
14. Wallace L, Williams R, Rea A, Croghan C. Continuous weeklong measurements of personal exposures and indoor concentrations of fine particles for 37 health-impaired North Carolina residents for up to four seasons. *Atmos Environ.* 2006;40:399-414.

15. Noris F, Adamkiewicz G, Delp WW, Hotchi T, Russell M, Singer BC, Spears M, Vermeer K, Fisk WJ. Indoor environmental quality benefits of apartment energy retrofits. *Build Environ.* 2013;68:170-178.
16. Morawska L, He CR, Hitchins J, Mengersen K, Gilbert D. Characteristics of particle number and mass concentrations in residential houses in Brisbane, Australia. *Atmos Environ.* 2003;37:4195-4203.
17. Allen R, Larson T, Sheppard L, Wallace L, Liu LJS. Use of real-time light scattering data to estimate the contribution of infiltrated and indoor-generated particles to indoor air. *Environ Sci Technol.* 2003;37:3484-3492.
18. Barn P, Larson T, Noullett M, Kennedy S, Copes R, Brauer M. Infiltration of forest fire and residential wood smoke: an evaluation of air cleaner effectiveness. *J Exposure Sci Environ Epidemiol.* 2008;18:503-511.
19. Brauer M, Hirtle R, Lang B, Ott W. Assessment of indoor fine aerosol contributions from environmental tobacco smoke and cooking with a portable nephelometer. *J Exposure Anal Environ Epidemiol.* 2000;10:136-144.
20. Jiang RT, Acevedo-Bolton V, Cheng KC, Klepeis NE, Ott WR, Hildemann LM. Determination of response of real-time SidePak AM510 monitor to secondhand smoke, other common indoor aerosols, and outdoor aerosol. *J Environ Monit.* 2011;13:1695-1702.
21. Dacunto PJ, Cheng KC, Acevedo-Bolton V, Jiang RT, Klepeis NE, Repace JL, Ott WR, Hildemann LM. Real-time particle monitor calibration factors and PM2.5 emission factors for multiple indoor sources. *Environmental Science-Processes & Impacts.* 2013;15:1511-1519.
22. Singer BC, Delp WW. Response of consumer and research grade indoor air quality monitors to residential sources of fine particles. *Indoor Air.* 2018;28:624-639.
23. Sousan S, Koehler K, Hallett L, Peters TM. Evaluation of consumer monitors to measure particulate matter. *J Aerosol Sci.* 2017;107:123-133.
24. Magi BI, Cupini C, Francis J, Green M, Hauser C. Evaluation of PM2.5 measured in an urban setting using a low-cost optical particle counter and a Federal Equivalent Method Beta Attenuation Monitor. *Aerosol Sci Technol.* 2019.
25. Holstius DM, Pillarisetti A, Smith KR, Seto E. Field calibrations of a low-cost aerosol sensor at a regulatory monitoring site in California. *Atmospheric Measurement Techniques.* 2014;7:1121-1131.
26. Gao ML, Cao JJ, Seto E. A distributed network of low-cost continuous reading sensors to measure spatiotemporal variations of PM2.5 in Xi'an, China. *Environ Pollut.* 2015;199:56-65.
27. Jiao W, Hagler G, Williams R, Sharpe R, Brown R, Garver D, Judge R, Caudill M, Rickard J, Davis M, Weinstock L, Zimmer-Dauphinee S, Buckley K. Community Air Sensor Network (CAIRSENSE) project: evaluation of low-cost sensor performance in a

suburban environment in the southeastern United States. *Atmospheric Measurement Techniques.* 2016;9:5281-5292.
28. Kelly KE, Whitaker J, Petty A, Widmer C, Dybwad A, Sleeth D, Martin R, Butterfield A. Ambient and laboratory evaluation of a low-cost particulate matter sensor. *Environ Pollut.* 2017;221:491-500.
29. Mukherjee A, Stanton LG, Graham AR, Roberts PT. Assessing the Utility of Low-Cost Particulate Matter Sensors over a 12-Week Period in the Cuyama Valley of California. *Sensors.* 2017;17.
30. Borghi F, Spinazze A, Campagnolo D, Rovelli S, Cattaneo A, Cavallo DM. Precision and Accuracy of a Direct-Reading Miniaturized Monitor in PM2.5 Exposure Assessment. *Sensors.* 2018;18.
31. Johnson KK, Bergin MH, Russell AG, Hagler GSW. Field Test of Several Low-Cost Particulate Matter Sensors in High and Low Concentration Urban Environments. *Aerosol and Air Quality Research.* 2018;18:565-578.
32. Zheng TS, Bergin MH, Johnson KK, Tripathi SN, Shirodkar S, Landis MS, Sutaria R, Carlson DE. Field evaluation of low-cost particulate matter sensors in high-and low-concentration environments. *Atmospheric Measurement Techniques.* 2018;11:4823-4846.
33. Cavaliere A, Carotenuto F, Di Gennaro F, Gioli B, Gualtieri G, Martelli F, Matese A, Toscano P, Vagnoli C, Zaldei A. Development of Low-Cost Air Quality Stations for Next Generation Monitoring Networks: Calibration and Validation of PM2.5 and PM10 Sensors. *Sensors.* 2018;18.
34. Crilley LR, Shaw M, Pound R, Kramer LJ, Price R, Young S, Lewis AC, Pope FD. Evaluation of a low-cost optical particle counter (Alphasense OPC-N2) for ambient air monitoring. *Atmospheric Measurement Techniques.* 2018;11:709-720.
35. Liu HY, Schneider P, Haugen R, Vogt M. Performance Assessment of a Low-Cost PM2.5 Sensor for a near Four-Month Period in Oslo, Norway. *Atmosphere.* 2019;10.
36. Sayahi T, Butterfield A, Kelly KE. Long-term field evaluation of the Plantower PMS low-cost particulate matter sensors. *Environ Pollut.* 2019;245:932-940.
37. Zamora ML, Xiong FLZ, Gentner D, Kerkez B, Kohrman-Glaser J, Koehler K. Field and Laboratory Evaluations of the Low-Cost Plantower Particulate Matter Sensor. *Environ Sci Technol.* 2019;53:838-849.
38. Tryner J, L'Orange C, Mehaffy J, Miller-Lionberg D, Hofstetter JC, Wilson A, Volckens J. Laboratory evaluation of low-cost PurpleAir PM monitors and in-field correction using co-located portable filter samplers. *Atmos Environ.* 2019;117067.
39. Papapostolou V, Zhang H, Feenstra BJ, Polidori A. Development of an environmental chamber for evaluating the performance of low-cost air quality sensors under controlled conditions. *Atmosheric Environment.* 2017;171:82-90.
40. Dacunto PJ, Klepeis NE, Cheng KC, Acevedo-Bolton V, Jiang RT, Repace JL, Otta WR, Hildemann LM. Determining PM2.5 calibration curves for a low-cost particle monitor:

common indoor residential aerosols. *Environmental Science-Processes & Impacts.* 2015;17:1959-1966.

41. Manikonda A, Zikova N, Hopke PK, Ferro AR. Laboratory assessment of low-cost PM monitors. *J Aerosol Sci.* 2016;102:29-40.
42. Zou Y, Young M, Wickey M, May A, Clark JD. Response of eight low-cost particle sensors and consumer devices to typical indoor emission events in a real home (ASHRAE 1756-RP). *Science and Technology for the Built Environment.* 2019;1-13.
43. Curto A, Donaire-Gonzalez D, Barrera-Gomez J, Marshall JD, Nieuwenhuijsen MJ, Wellenius GA, Tonne C. Performance of low-cost monitors to assess household air pollution. *Environ Res.* 2018;163:53-63.
44. Wang Y, Li JY, Jing H, Zhang Q, Jiang JK, Biswas P. Laboratory Evaluation and Calibration of Three Low- Cost Particle Sensors for Particulate Matter Measurement. *Aerosol Sci Technol.* 2015;49:1063-1077.
45. Sousan S, Koehler K, Thomas G, Park JH, Hillman M, Halterman A, Peters TM. Inter-comparison of low-cost sensors for measuring the mass concentration of occupational aerosols. *Aerosol Sci Technol.* 2016;50:462-473.
46. Morawska L, Thai PK, Liu XT, Asumadu-Sakyi A, Ayoko G, Bartonova A, Bedini A, Chai FH, Christensen B, Dunbabin M, Gao J, Hagler GSW, Jayaratne R, Kumar P, Lau AKH, Louie PKK, Mazaheri M, Ning Z, Motta N, Mullins B, Rahman MM, Ristovski Z, Shafiei M, Tjondronegoro D, Westerdahl D, Williams R. Applications of low-cost sensing technologies for air quality monitoring and exposure assessment: How far have they gone? *Environ Int.* 2018;116:286-299.
47. Rai AC, Kumar P, Pilla F, Skouloudis AN, Di Sabatino S, Ratti C, Yasar A, Rickerby D. End-user perspective of low-cost sensors for outdoor air pollution monitoring. *Sci Total Environ.* 2017;607:691-705.

SUPPLEMENTARY MATERIAL

Performance of low-cost indoor air quality monitors for $PM_{2.5}$ and PM_{10} from residential sources

Zhiqiang Wang[1], Woody W. Delp[2], Brett C. Singer[2*],

[1] Tianjin Key Lab of Refrigeration, Tianjin University of Commerce, Tianjin, China
[2] Indoor Environment Group and Residential Building Systems Group, Lawrence Berkeley National Laboratory, Berkeley, CA, USA
*Corresponding email: bcsinger@lbl.gov

TEOM Data Collection and Processing

A Tapered Element Oscillating Microbalance with Filter Dynamic Measurement System Model 1405-DF (Thermo Fisher Scientific), henceforth TEOM, was used as a reference $PM_{2.5}$ monitor. The TEOM is designed to provide hourly resolved data for ambient air monitoring, which is developed from measurements that occur over shorter intervals. For 6 minutes the TEOM operates in a Base measurement mode in which sample air is heated to 30ºC then pulled through a filter affixed to an oscillating element. As particles are collected on the filter, the oscillation frequency changes and the collected mass is calculated. During the next 6 minutes, the TEOM operates in a Reference mode, in which sample air is cooled and passed through the filter on the oscillating element. The filtering and cooling process is designed to remove both particle and semi-volatile gases that can be collected on the filter and bias PM measurements. Any change in oscillation that occurs during the Reference measurement is assumed to be caused by the loss of semi-volatile gases that can bias the PM measurement. The concentration is the base measurement minus the reference measurement. During and following events with significant volatile fractions the reference measurement can be negative, due to the fact that this clean volatile particle free air is driving off previously collected mass.

The TEOM was configured to report out the Base and Reference measurements every 6 minutes. The Base measurements are only updated each 12 minutes (as the Reference measurements are updated on the alternating 12 min cycle). This is highly resolved for outdoors but not fast or resolved enough for indoor sources. Thus, in our processing of TEOM data, we first imputed Base values for each time step that had a repeated value of the Base reading (when the device was in Reference mode). We then subtracted the Reference measurement from the imputed Base value to calculate an estimated $PM_{2.5}$ concentration for each 6-min time step. An example of this is provided in Figure 1.

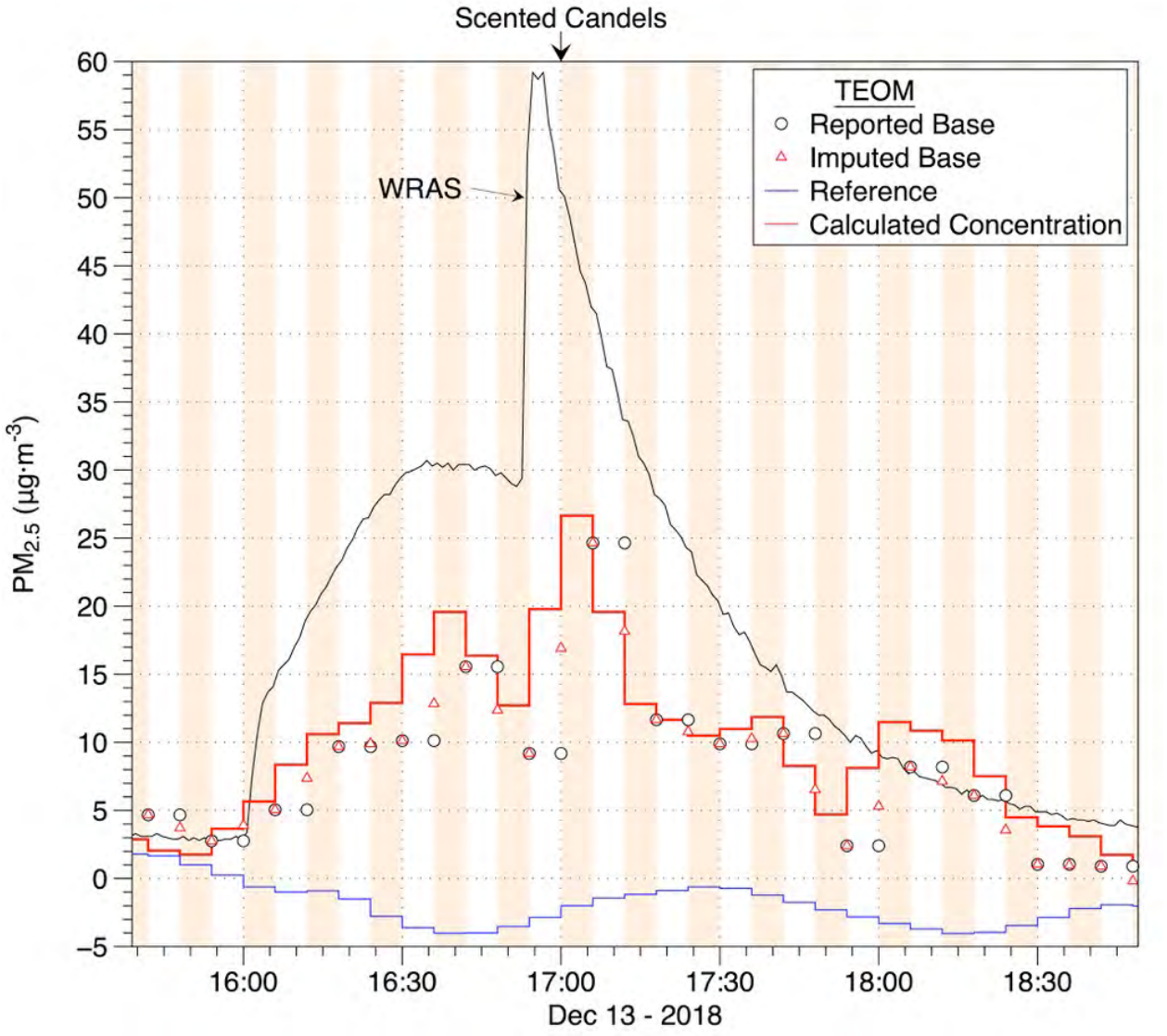


Figure S1. Example of raw data and processing to estimate 6-min resolved $PM_{2.5}$ concentration for the TEOM-FDMS.

Table S1. Mass concentration measured for experiments that included filter sampling

Event	Date	Timing of filter sample collection [1]	Filter $PM_{2.5}$ $\mu g/m^3$	WRAS $PM_{2.5}$ $\mu g/m^3$	WRAS/ Filter $PM_{2.5}$	Filter PM_{10} $\mu g/m^3$	WRAS PM_{10} $\mu g/m^3$	WRAS/ Filter PM_{10}
Humidifier 1	12/10/2018	10:33-11:30	52.5	36.5	0.7	52.5	38.9	0.7
Humidifier 2	12/10/2018	13:00-14:45	89.0	73.2	0.8	103.8	76.1	0.7
Microwave popcorn	12/11/2018	10:15-11:15	36.8	47.0	1.3	41.6	64.3	1.5
Incense stick 1	12/11/2018	13:15-14:15	115.3	156.6	1.4	100.1	157.6	1.6
Toast white bread	12/12/2018	9:15-10:15	23.8	59.4	2.5	28.3	60.7	2.1
E-grilled burger	12/12/2018	12:15-13:15	49.7	93.6	1.9	58.8	103.8	1.8
Mosquito coil 1	12/12/2018	15:15-16:15	60.3	94.4	1.6	72.0	95.8	1.3
Boiled potatoes	12/13/2018	7:56-9:54	4.3	12.1	2.8	10.9	14.9	1.4
Unscented candles	12/13/2018	11:39-12:34	58.1	96.5	1.7	62.5	101.0	1.6
Snuff candles	12/13/2018	12:35-13:35	74.5	123.6	1.7	76.5	127.4	1.7
Scented candles	12/13/2018	15:57-16:51	16.2	23.3	1.4	17.3	23.4	1.4
Snuff candles	12/13/2018	16:53-17:33	31.8	35.1	1.1	34.5	37.9	1.1
Broil Br. sprouts	12/14/2018	8:18-9:48	24.0	68.0	2.8	27.3	70.8	2.6
Arizona test dust	12/14/2018	11:45-13:05	45.1	32.3	0.7	73.8	118.3	1.6
Stir-fry spinach	12/14/2018	14:15-15:48	70.3	87.7	1.2	103.8	113.9	1.1
Mosquito coil 2	12/14/2018	17:05-18:05	66.8	96.0	1.4	66.8	96.9	1.5
Heat olive oil	12/17/2018	8:06-9:45	24.4	46.5	1.9	29.1	48.2	1.7
Vacuum	12/17/2018	11:45-13:15	49.9	29.0	0.6	117.9	56.5	0.5
Pan-fry eggs	12/17/2018	17:00-17:50	102.8	144.8	1.4	182.8	163.6	0.9
Pan-fry bacon	12/18/2018	7:48-10:12	177.0	248.5	1.4	189.0	261.4	1.4
Pan-fry fish	12/18/2018	10:58-12:55	14.4	26.7	1.8	30.2	32.1	1.1
Broil bacon	12/18/2018	13:30-15:00	27.5	77.2	2.8	30.2	79.4	2.6
Incense stick 2	12/18/2018	16:15-17:15	216.6	216.2	1.0	208.7	216.5	1.0
Broil potatoes	12/19/2018	7:44-9:15	49.6	139.1	2.8	56.9	140.8	2.5

[1] Generally started just before the initiation of the particle-generating activity.

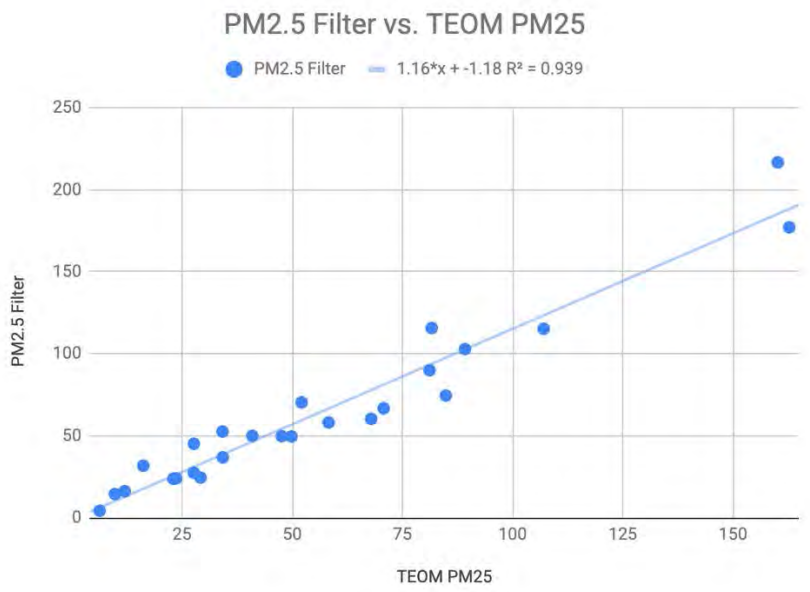


Figure S2. Correlation of PM2.5 measured with gravimetric samples to time-correlated measurements with the TEOM-FDMS.

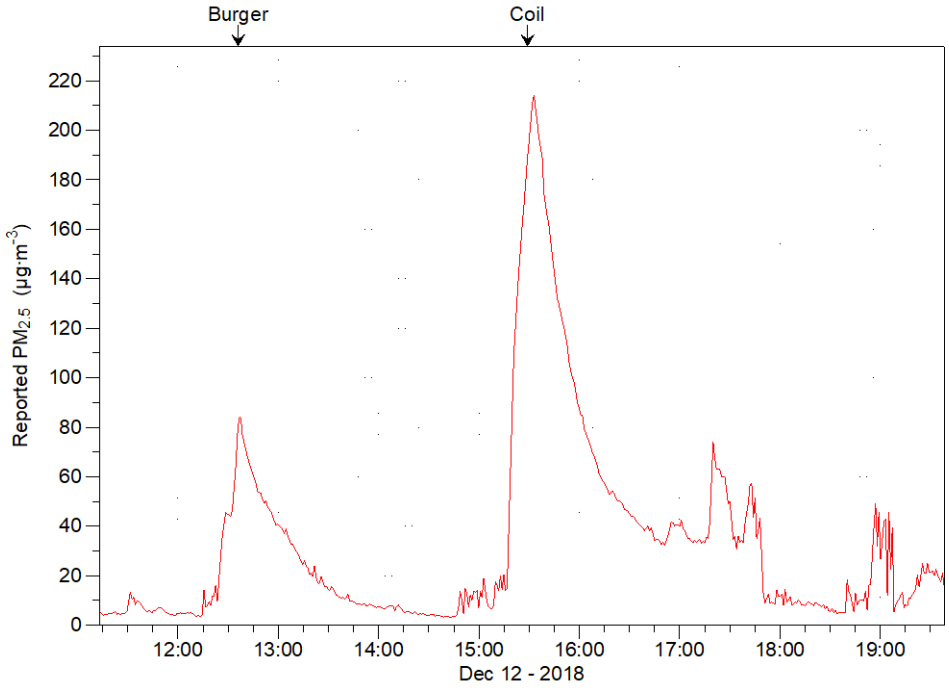


Figure S3. Example data from three AQE devices revealing one intermittently bad sensor.

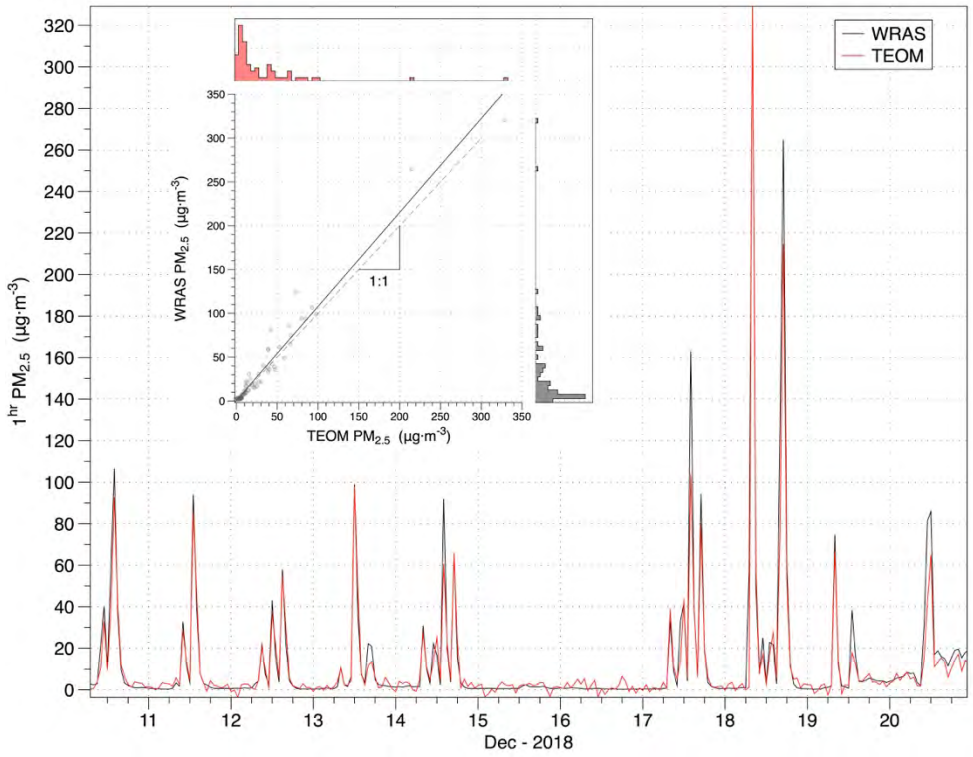


Figure S4. Comparison of Adjusted WRAS and TEOM hourly $PM_{2.5}$ over the entire experimental period.

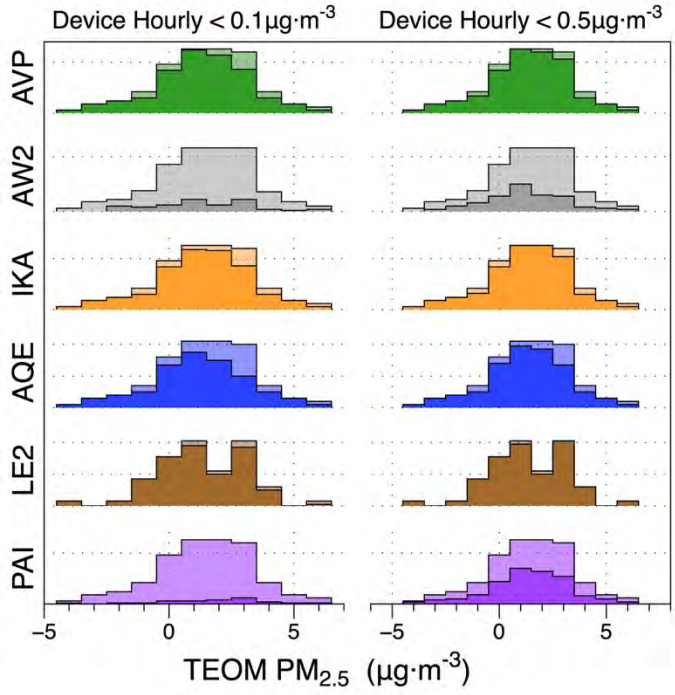


Figure S5. Distribution of hourly TEOM $PM_{2.5}$ concentrations measured in the experimental room during overnight periods (no source) with HEPA-filtered supply air.

Table S2. Parameters for linear fits shown in Figure 2 in the main manuscript.

	Intercept	Slope	R^2
AQE	-4.516	2.758	0.785
AVP	-2.714	1.258	0.776
AW2	-1.668	1.260	0.776
IKA	-2.961	1.468	0.799
LE2	-4.845	1.707	0.746
PA	-1.444	1.923	0.760

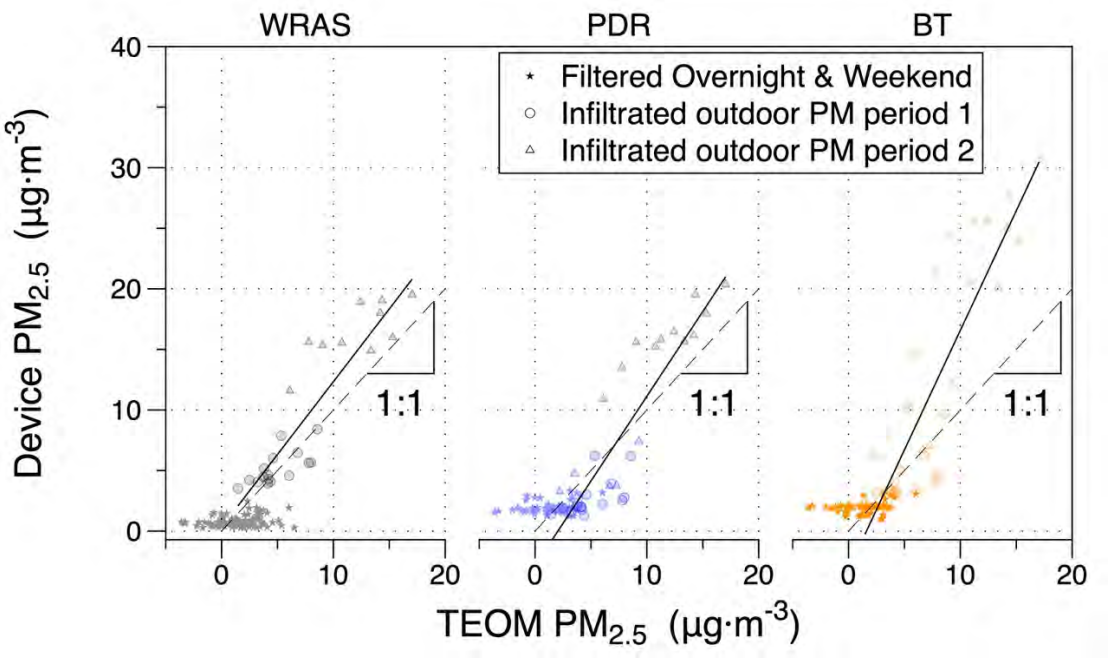


Figure S6. Hourly $PM_{2.5}$ reported by professional grade monitors and the TEOM during overnight periods with the room open to outdoor air and no filtration and during no-source periods with filtered supply air.

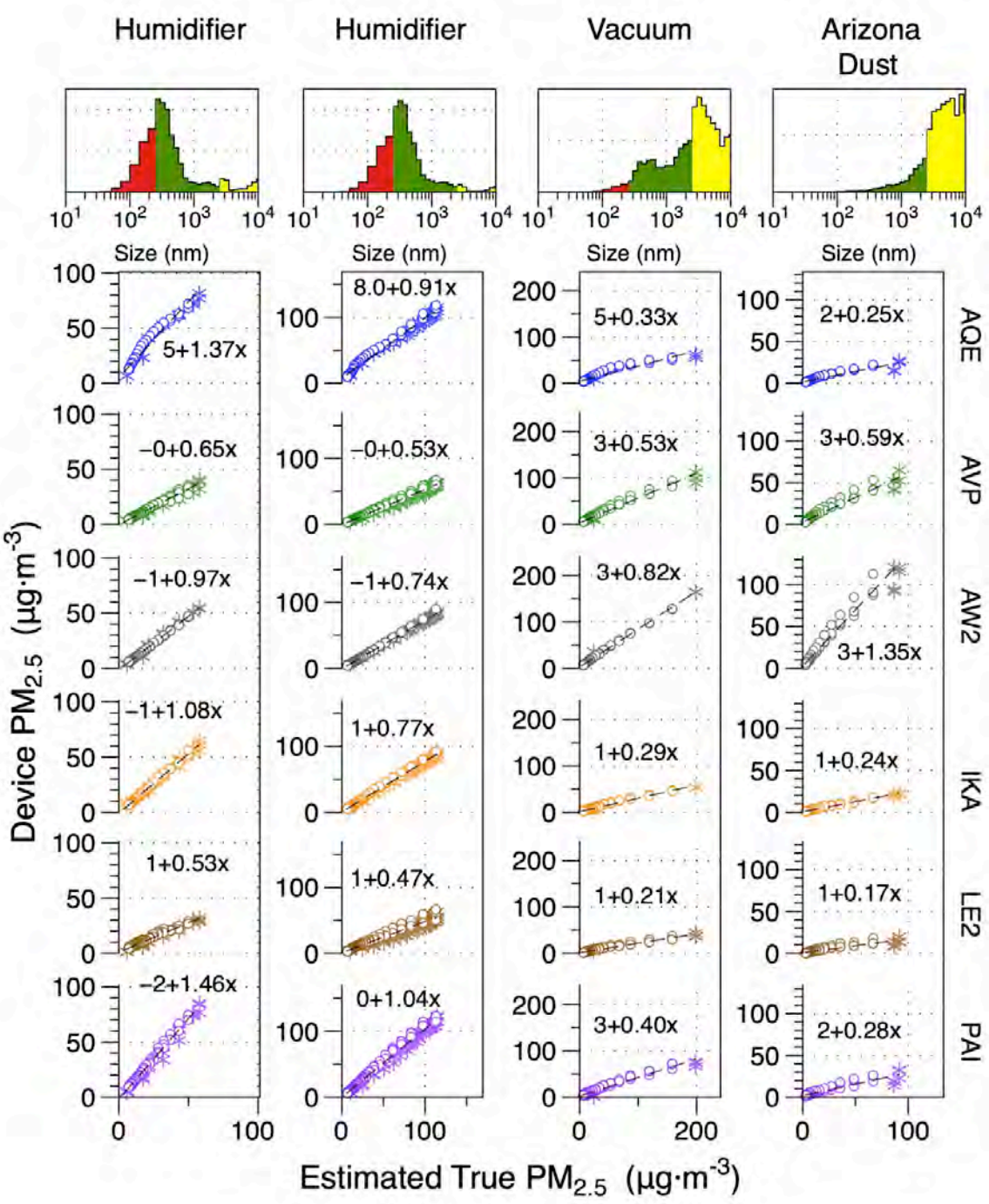


Figure S7. Correlations between 5-min average $PM_{2.5}$ reported by low-cost monitors and estimated true $PM_{2.5}$ from WRAS adjusted to gravimetric data for mineral sources. Histograms at top show the distribution of PM mass over range of 10 nm to 10 µm.

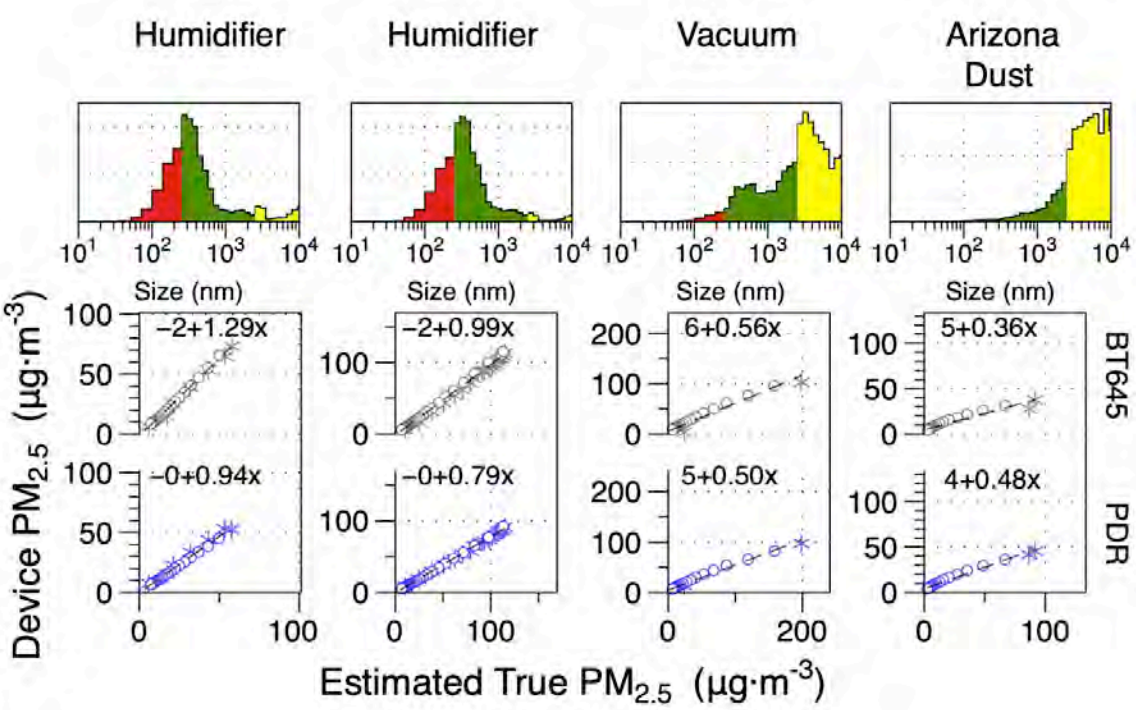


Figure S8. Correlations of 5-min average $PM_{2.5}$ reported for professional monitors with estimated true $PM_{2.5}$ from WRAS adjusted to gravimetric data for mineral sources.

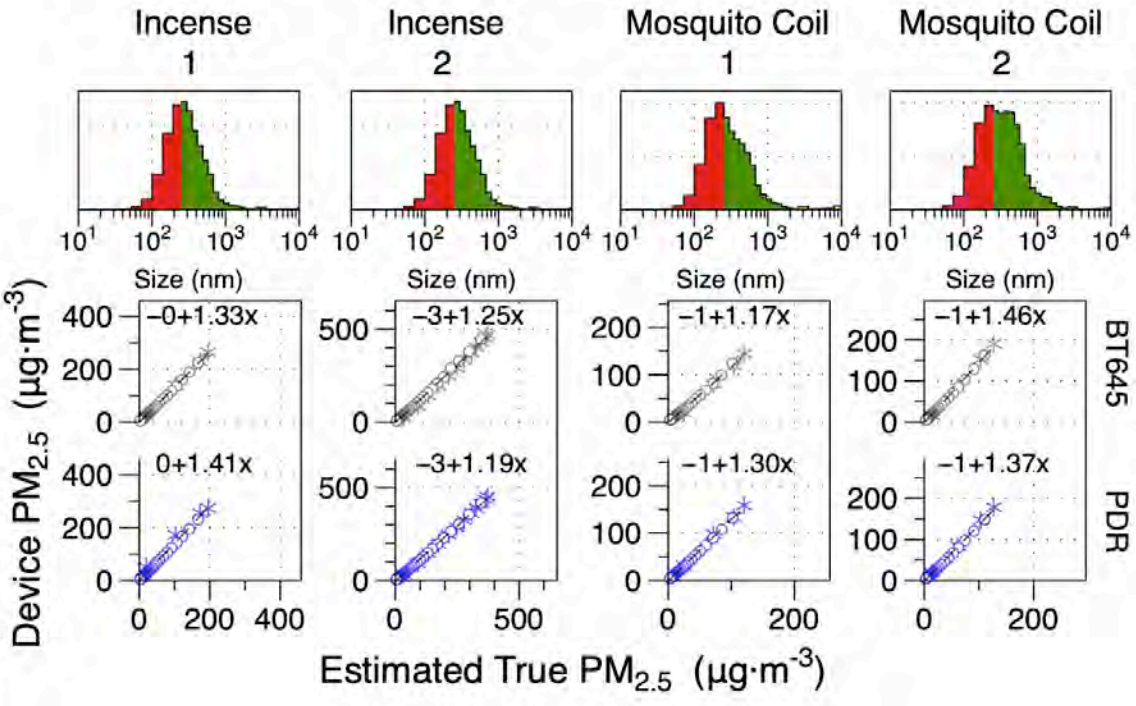


Figure S9. Correlations of 5-min average $PM_{2.5}$ reported for professional monitors with estimated true $PM_{2.5}$ from WRAS adjusted to gravimetric data for incense and mosquito coil sources.

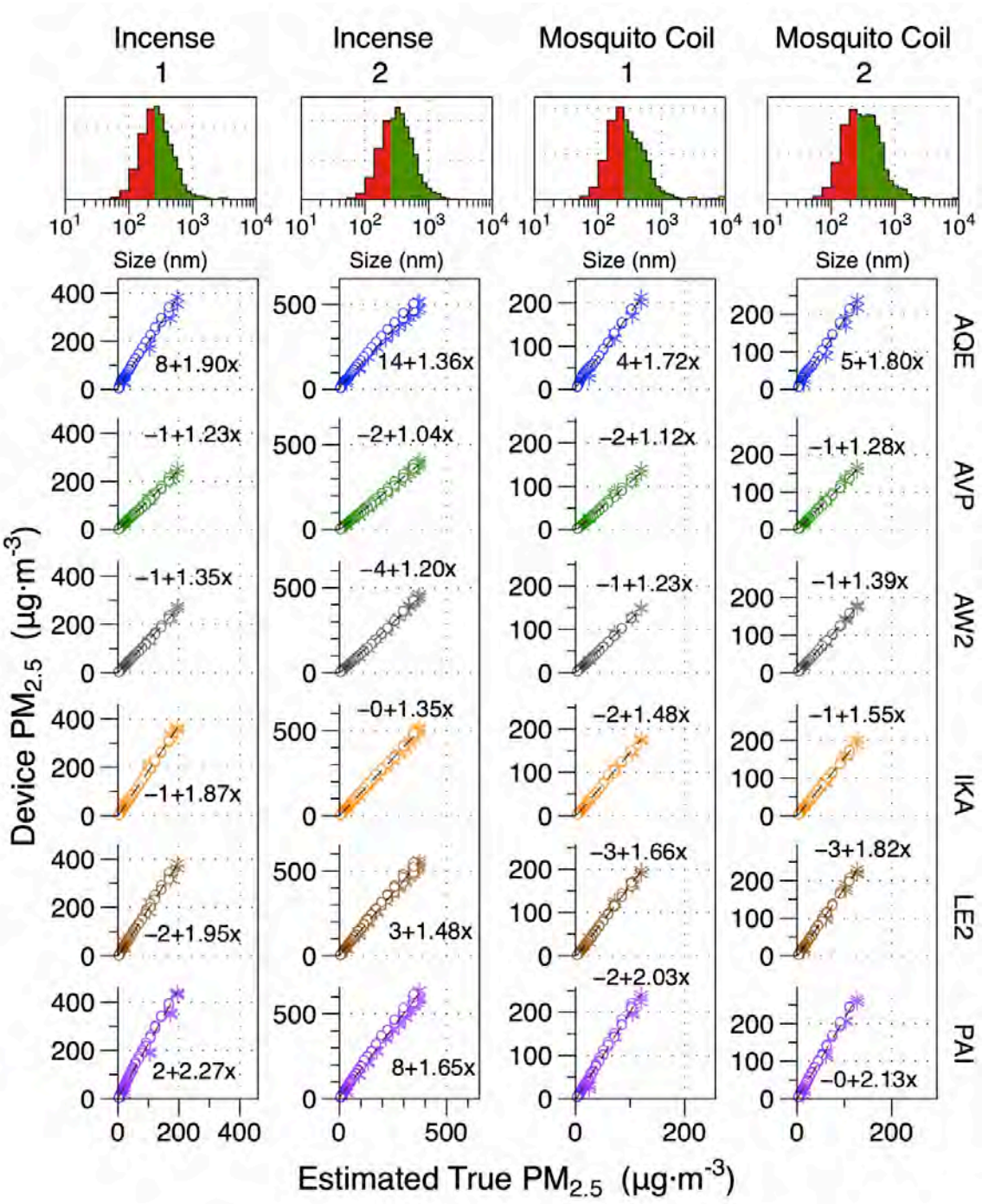


Figure S10. Correlations between 5-min average $PM_{2.5}$ reported by low-cost monitors and estimated true $PM_{2.5}$ from WRAS adjusted to gravimetric data for incense and mosquito coil. Histograms at top show the distribution of PM mass over range of 10 nm to 10 µm.

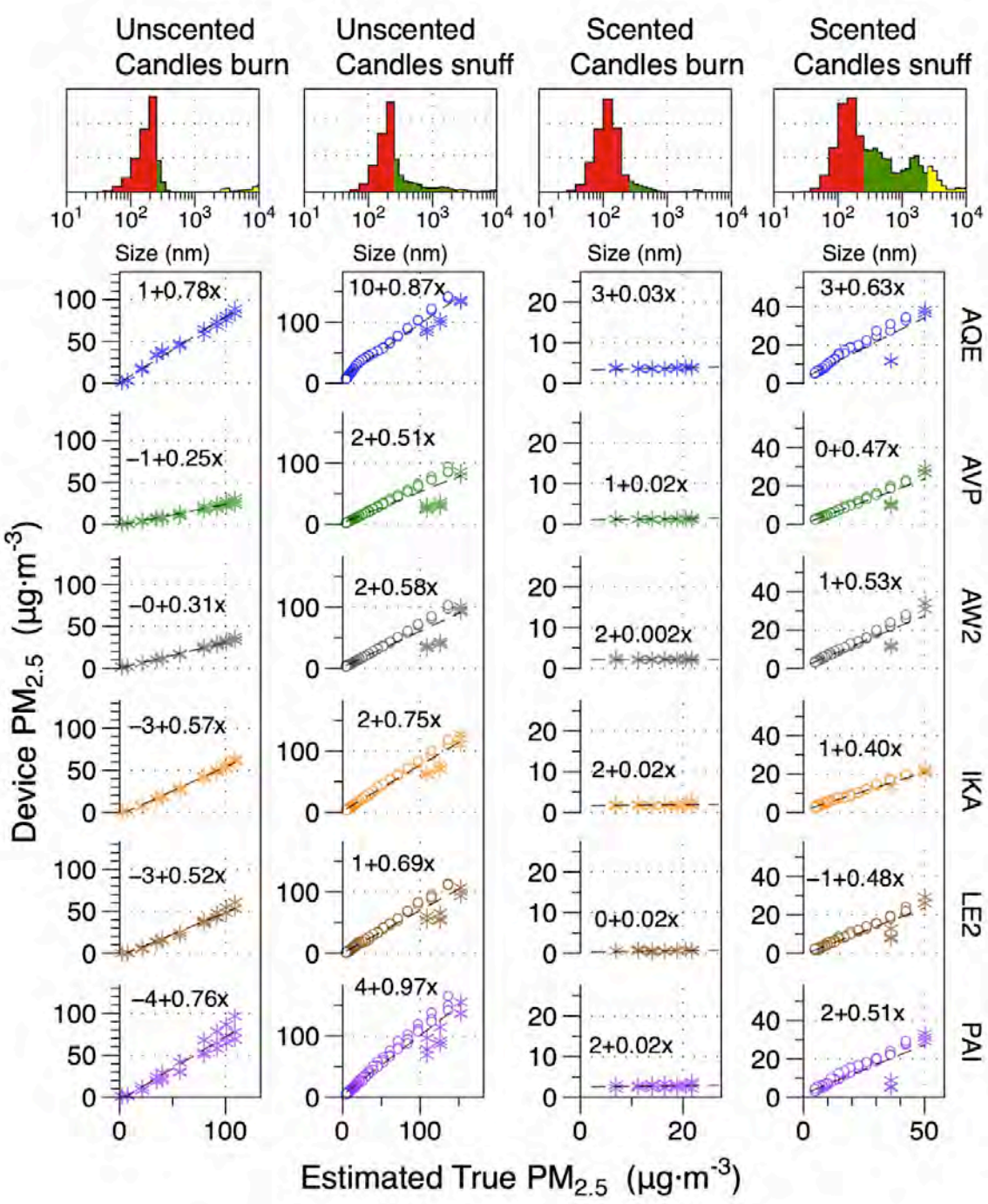


Figure 11. Correlations between 5-min average PM2.5 reported by low-cost monitors and estimated true PM2.5 from WRAS adjusted to gravimetric data for candles under steady burn and after being extinguished (snuff). Histograms at top show the distribution of PM mass over range of 10 nm to 10 □m.

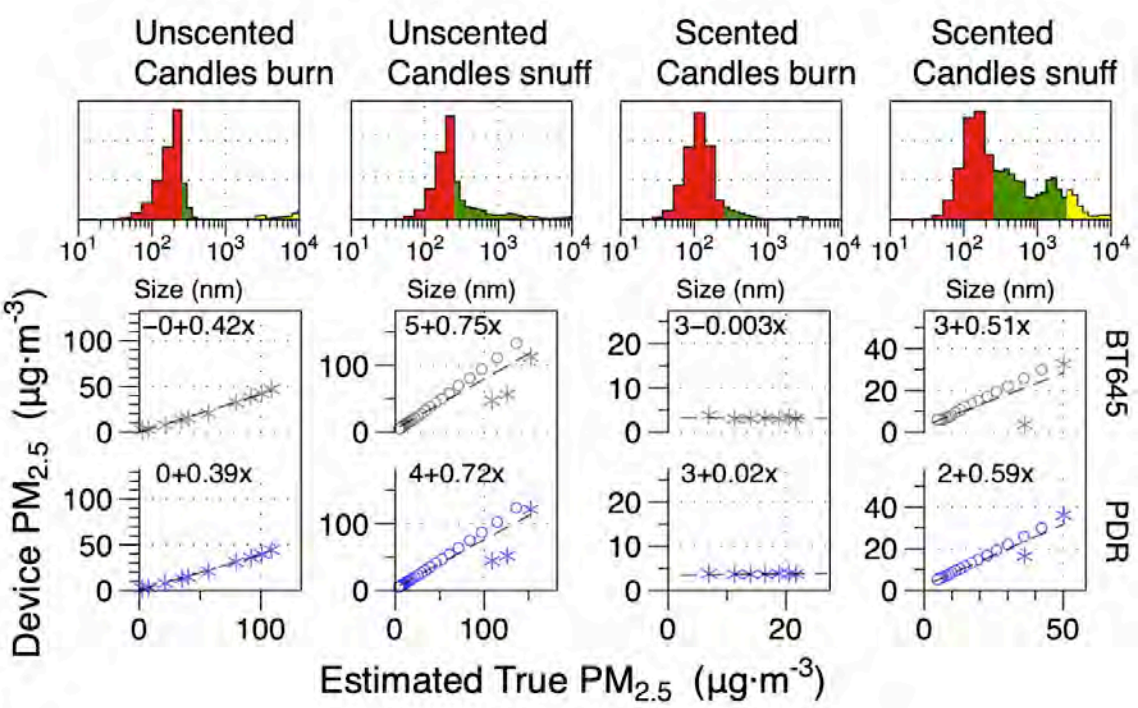


Figure S12. Linear correlations of 5-min average $PM_{2.5}$ reported for professional monitors with estimated true $PM_{2.5}$ from WRAS adjusted to gravimetric data for candles.

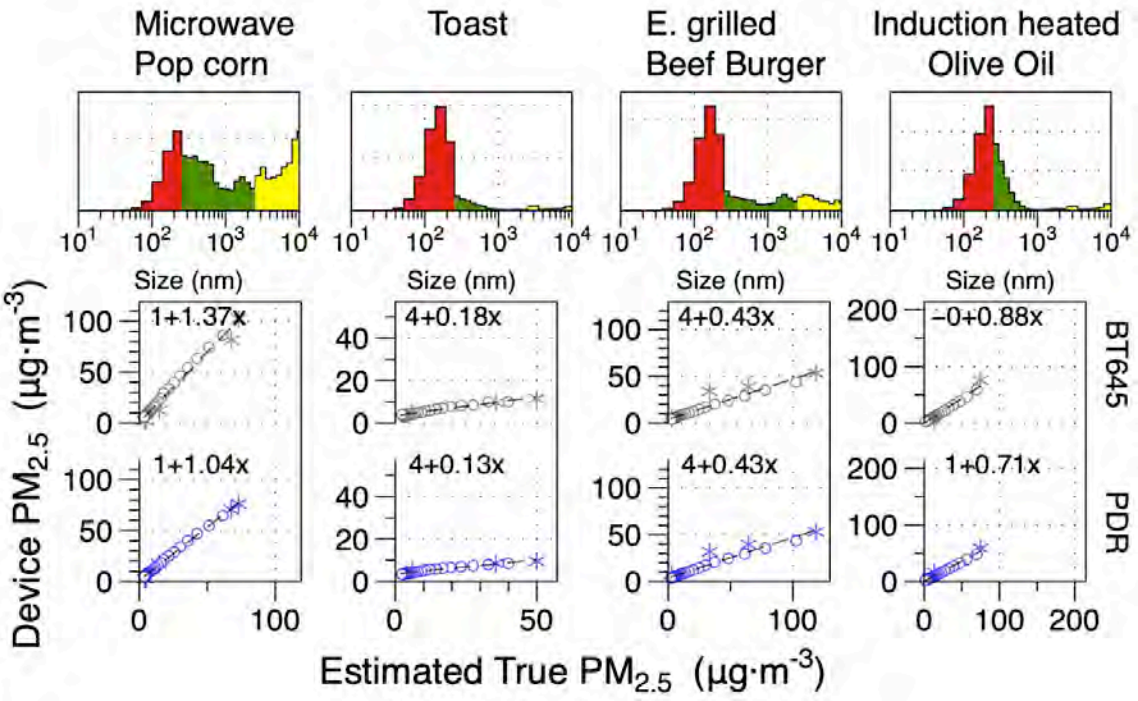


Figure S13. Linear correlations of 5-min average $PM_{2.5}$ reported for professional monitors with estimated true $PM_{2.5}$ from WRAS adjusted to gravimetric data for electric cooking.

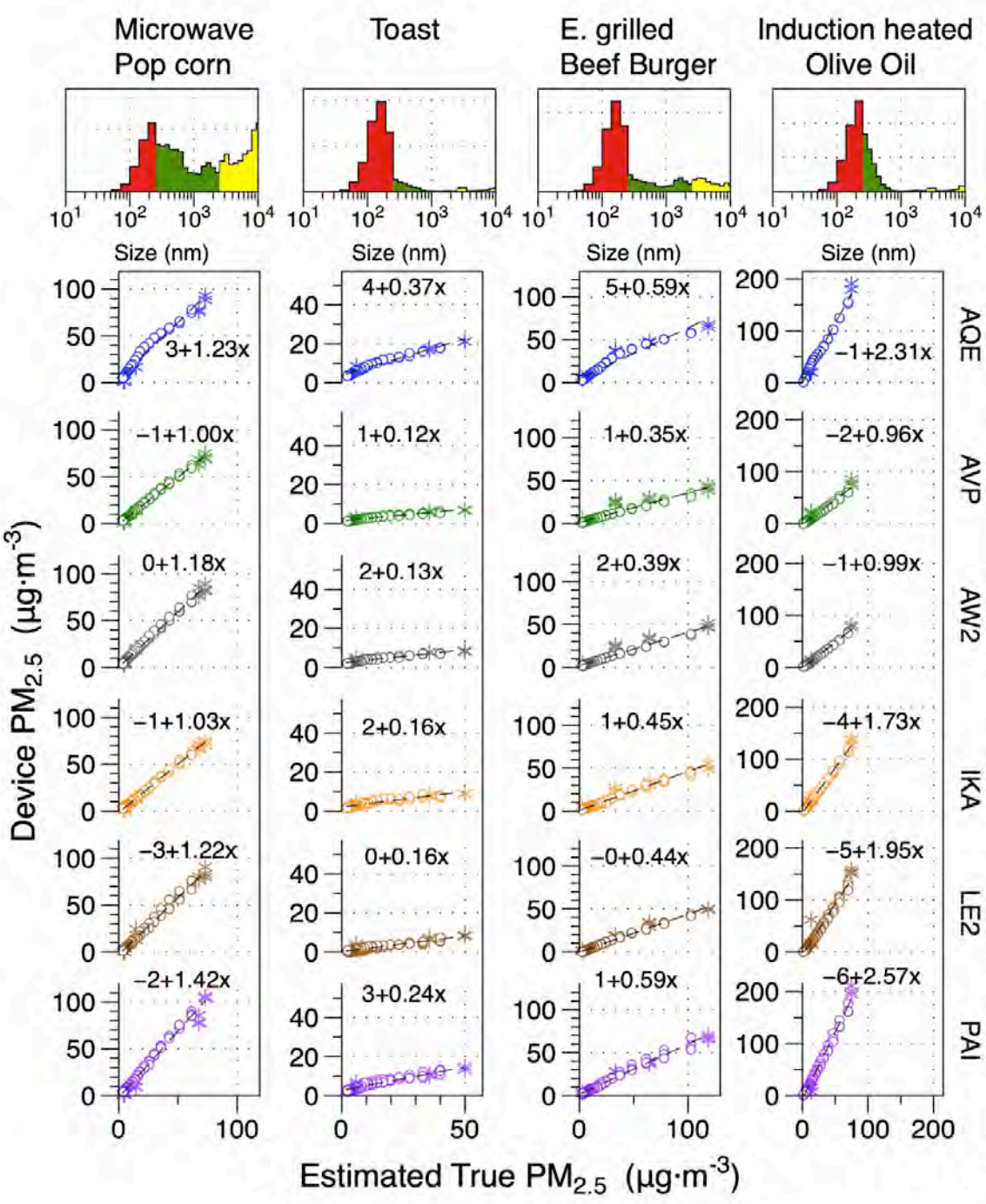


Figure 14. Correlations between 5-min average $PM_{2.5}$ reported by low-cost monitors and estimated true $PM_{2.5}$ from WRAS adjusted to gravimetric data for electric cooking. Histograms at top show the distribution of PM mass over range of 10 nm to 10 µm.

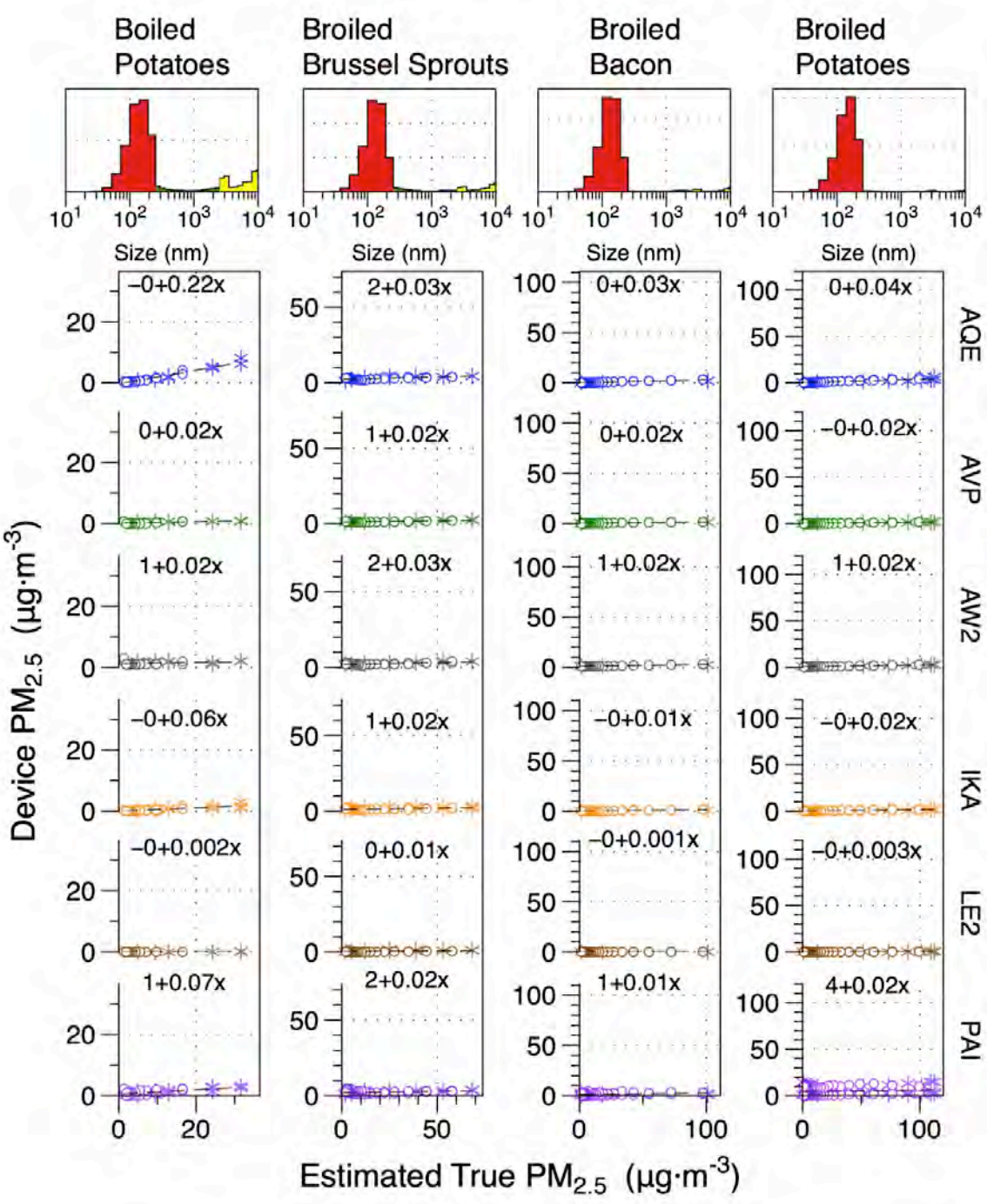


Figure 15. Correlations between 5-min average PM2.5 reported by low-cost monitors and estimated true PM2.5 from WRAS adjusted to gravimetric data for gas cooking without frying. Histograms at top show the distribution of PM mass over range of 10 nm to 10 □m.

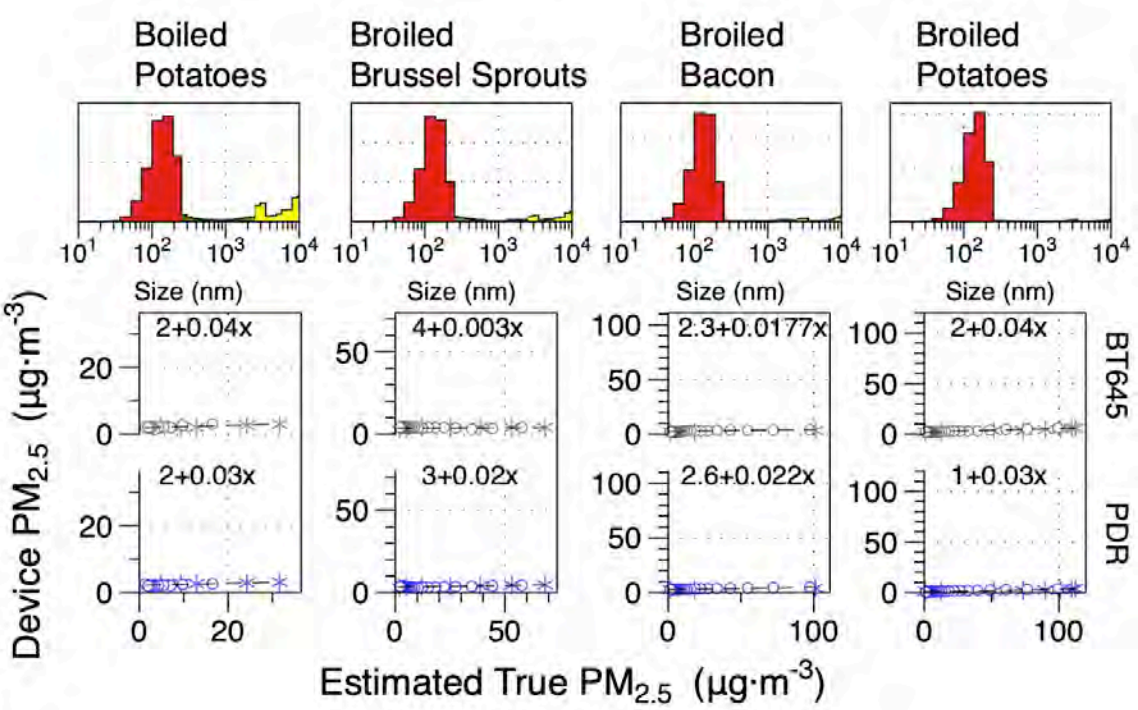


Figure S16. Linear correlations of 5-min average $PM_{2.5}$ reported for professional monitors with estimated true $PM_{2.5}$ from WRAS adjusted to gravimetric data for gas cooking without frying.

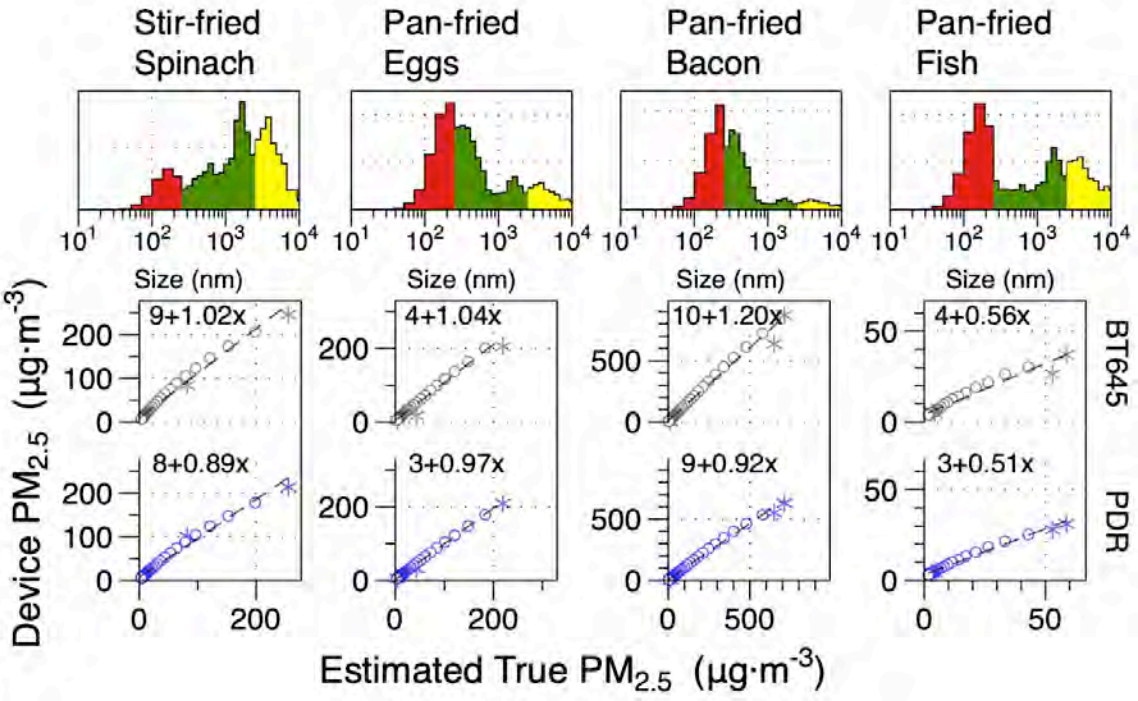


Figure S17. Linear correlations of 5-min average $PM_{2.5}$ reported for professional monitors with estimated true $PM_{2.5}$ from WRAS adjusted to gravimetric data for cooking by frying and stir-frying.

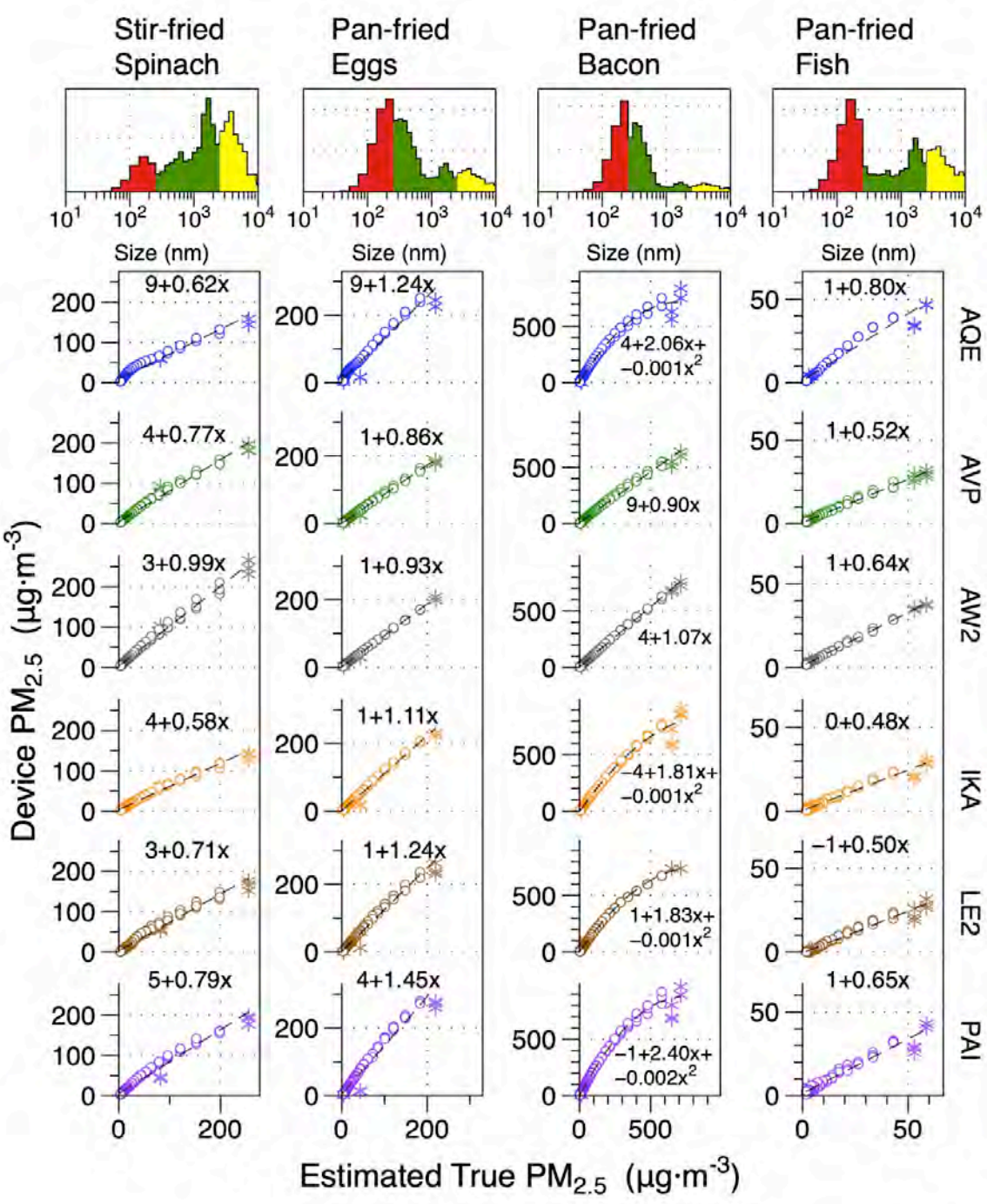


Figure 18. Correlations between 5-min average $PM_{2.5}$ reported by low-cost monitors and estimated true $PM_{2.5}$ from WRAS adjusted to gravimetric data for cooking by frying and stir-frying. Histograms at top show the distribution of PM mass over range of 10 nm to 10 µm.